EUROPEAN RESPIRATORY *journal*

FLAGSHIP SCIENTIFIC JOURNAL OF ERS

Early View

Original article

Profibrotic function of pulmonary group 2 innate lymphoid cells is controlled by Regnase-1

Yoshinari Nakatsuka, Ai Yaku, Tomohiro Handa, Alexis Vandenbon, Yuki Hikichi, Yasutaka Motomura, Ayuko Sato, Masanori Yoshinaga, Kiminobu Tanizawa, Kizuku Watanabe, Toyohiro Hirai, Kazuo Chin, Yutaka Suzuki, Takuya Uehata, Takashi Mino, Tohru Tsujimura, Kazuyo Moro, Osamu Takeuchi

Please cite this article as: Nakatsuka Y, Yaku A, Handa T, *et al*. Profibrotic function of pulmonary group 2 innate lymphoid cells is controlled by Regnase-1. *Eur Respir J* 2020; in press (https://doi.org/10.1183/13993003.00018-2020).

Profibrotic function of pulmonary group 2 innate lymphoid cells is controlled by Regnase-1

Yoshinari Nakatsuka[1,2], Ai Yaku[2,3], Tomohiro Handa[4], Alexis Vandenbon[5], Yuki Hikichi[6], Yasutaka Motomura[7], Ayuko Sato[8], Masanori Yoshinaga[2], Kiminobu Tanizawa[9], Kizuku Watanabe[9], Toyohiro Hirai[9], Kazuo Chin[1], Yutaka Suzuki[10], Takuya Uehata[2], Takashi Mino[2], Tohru Tsujimura[8], Kazuyo Moro[6,7], and Osamu Takeuchi[2]*.

[1]Department of Respiratory Care and Sleep Medicine, Graduate School of Medicine, Kyoto University, Kyoto, Japan; [2]Department of Medical Chemistry, Graduate School of Medicine, Kyoto University, Kyoto, Japan; [3]Department of Rheumatology and Clinical Immunology, Graduate School of Medicine, Kyoto University, Kyoto, Japan; [4]Department of Advanced Medicine for Respiratory Failure, Graduate School of Medicine, Kyoto University, Kyoto, Japan.; [5]Laboratory of Systems Virology, Department of Biosystems Science, Institute for Frontier Life and Medical Sciences, Kyoto University, Kyoto, Japan; [6]Laboratory for Innate Immune Systems, RIKEN Center for Integrative Medical Sciences, Kanagawa, Japan; [7]Department of Microbiology and Immunology, Osaka University Graduate School of Medicine, Osaka, Japan.; [8]Department of Pathology, Hyogo College of Medicine, Hyogo, Japan.; [9]Department of Respiratory Medicine, Graduate School of Medicine, Kyoto University, Kyoto, Japan.; [10]Laboratory of Functional Genomics, Department of Medical Genome Sciences, Graduate School of Frontier Sciences, The University of Tokyo, Chiba, Japan.

* Corresponding author:

Osamu Takeuchi

Department of Medical Chemistry, Graduate School of Medicine, Kyoto University

Yoshida-Konoe-cho, Sakyo-ku, Kyoto 606-8501, Japan.

Phone: +81-75-753-9500 Fax: +81-75-753-9502

E-mail: otake@mfour.med.kyoto-u.ac.jp

Take home message

Regnase-1 controls the proliferation and activation of ILC2, which thereby attenuates lung fibrosis in mice. In humans, lower Regnase-1 level correlates with more abundant ILC2 number, which potentially associates with the prognosis of IPF patients.

Running title

Regnase-1 controls pro-fibrotic function of ILC2

Key words

Regnase-1, Group 2 innate lymphoid cells, Idiopathic pulmonary fibrosis, Prognosis

Abstract

Regnase-1 is an RNase critical for posttranscriptional control of pulmonary immune homeostasis in mice by degrading immune-related mRNAs. However, little is known about the cell types Regnase-1 controls in the lung, and its relevance to human pulmonary diseases.

Regnase-1-dependent changes in lung immune cell types were examined by a competitive bone marrow transfer mouse model, and group 2 innate lymphoid cells (ILC2s) were identified. Then the associations between Regnase-1 in ILC2s and human diseases were investigated by transcriptome analysis and a bleomycin-induced pulmonary fibrosis mouse model. The clinical significance of Regnase-1 in ILC2s was further assessed using patients-derived cells.

Regnase-1-deficiency resulted in the spontaneous proliferation and activation of ILC2s in the lung. Intriguingly, genes associated with pulmonary fibrosis were highly upregulated in *Regnase1*-deficient ILC2s compared with wild-type, and supplementation of *Regnase-1*-deficient ILC2s augmented bleomycin-induced pulmonary fibrosis in mice. Regnase-1 suppresses mRNAs encoding transcription factors *Gata3* and *Egr1*, which are potent to regulate fibrosis-associated genes. Clinically, Regnase-1 protein levels in ILC2 negatively correlated with the ILC2 population in bronchoalveolar lavage (BAL) fluid. Furthermore, idiopathic pulmonary fibrosis (IPF) patients with more than 1500 cells/ml peripheral blood ILC2s exhibited poorer prognosis than patients with lower numbers, implying the contribution of Regnase-1 in ILC2s for the progression of IPF.

Collectively, Regnase-1 was identified as a critical posttranscriptional regulator of the pro-fibrotic function of ILC2s both in mouse and human, suggesting that Regnase-1 may be a novel therapeutic target for IPF.

Introduction

A variety of immune cell types resides in the lung, and they coordinately eliminate pathogens or enhance recovery from the injury[1]. Immune cells are regulated through transcriptional and posttranscriptional mechanisms[2, 3]. Regnase-1, also known as ZC3H12A or MCPIP1, is vital for posttranscriptional immune regulation by acting as an RNase degrading mRNA such as *Il6* or *Icos* through the recognition of stem-loop structures in its 3′ untranslated regions (3′ UTR)[4-6]. Regnase-1 deficiency in mice results in the aberrant activation of immune cells and development of systemic inflammatory diseases[4]. Particularly, *Regnase-1*-deficient mice show a massive infiltration of various immune cells in the lungs[4, 7, 8]. However, cells intrinsically regulated by Regnase-1 remain unclear except for a study showing its role in the activation of Th2 cells and allergic inflammation via *Gata3* regulation[7]. In humans, decreased Regase-1 expression potentially contributes to the pathogenesis of psoriasis[9] and enhanced antitumor T cell activity[10]. However, little is known about the clinical significance of Regnase-1 in the lungs.

Dysregulation of the immune system causes a number of pulmonary disorders such as asthma and pneumonia[1]. In addition, the immune system contributes to the progression of pulmonary fibrotic diseases including idiopathic pulmonary fibrosis (IPF) [11]. Particularly, type 2 immunity plays an important role in IPF through the production of cytokines including IL-4, IL-5 and IL-13[12, 13]. These cytokines act on the fibroblasts to enhance collagen production and promote fibrosis. However, immune cell types responsible for the progression of fibrosis are yet to be clarified.

Group 2 innate lymphoid cells (ILC2s) were reported to be major sources of IL-5 and IL-13 in the lungs[14, 15]. Owing to this cytokine-producing capacity, ILC2s largely contribute to the development of bronchial asthma[16, 17]. In addition, recent studies implied that ILC2s are involved in the pathogenesis of pulmonary fibrosis[17-20]. However, the role

of ILC2s in pulmonary fibrosis and their regulatory mechanisms are largely unknown.

In this study, we investigated cell types intrinsically regulated by Regnase-1 in the lung, and discovered ILC2s. Lack of Regnase-1 in ILC2s worsened experimental pulmonary fibrosis, consistent with the control of genes related to pulmonary fibrosis by Regnase-1 in ILC2s. Furthermore, the human Regnase-1 protein levels inversely correlated with the number of ILC2s in the bronchoalveolar lavage (BAL), and the increased number of blood ILC2s was an independent factor for poor prognosis in IPF patients.

Methods

Mice and cell lines

Regnase-1$^{-/-}$, *Rag2*$^{-/-}$, *Il2rg*$^{-/-}$ and CD45.1 congenic mice were previously described[4, 5, 21, 22]. *Regnase-1*$^{-/-}$ mice and CD45.1 congenic mice were maintained on a C57BL/6 background. *Regnase-1*$^{-/-}$ mice crossed with *Rag2*$^{-/-}$ (*Regnase-1*$^{-/-}$*Rag2*$^{-/-}$) and *Rag2*$^{-/-}$ mice crossed with *Il2rg*$^{-/-}$ (*Rag2*$^{-/-}$*Il2rg*$^{-/-}$) mice were generated and maintained on a Balb/c background. All mice were grown under specific pathogen-free environments, and mice at ages between 7 and 12 weeks were subjected to the analysis. The sex of mice is summarized in supplementary table S1. The animal experiments were performed with the permission from the Kyoto University Animal Experimentation Committee (120002). *Regnase-1*-deficient and parental Jurkat cells were described previously[23].

Clinical study design

We performed an observational cohort study which included consecutive patients who were diagnosed as IPF at Kyoto University Hospital from May 2013 to February 2018. The diagnosis of IPF was made according to the international guideline[24] and confirmed to meet the current criteria[25]. Patients who had complications of acute infection, acute exacerbation of IPF, pneumothorax or active malignancies at the time of sample collection were excluded from the study. The day of sample collection was set as the baseline. For the analyses of ILC2s in the BAL, the patients who underwent BAL screening as a systemic evaluation under the suspicion of sarcoidosis and were proven to have no abnormality in the lung were included as control subjects. The study was approved by the Kyoto University Hospital Institutional Review Board (G0296 and G1059).

Further details of experimental methods, clinical data collection and statistical analyses are described in the supplementary material.

Results

Regnase-1 deficiency drastically increases lung ILC2s in a cell-intrinsic manner

To identify the lung immune cell populations that are cell-intrinsically controlled by Regnase-1, we took advantage of the competitive bone marrow (BM) transfer model (supplementary method and supplementary figure S1A). The proportion of CD45.2 *Regnase-1*$^{-/-}$ ILC2s (defined as lineage^{-}CD45^{+}T1/ST2^{+}Sca-1^{+}KLRG1^{+} lymphocytes, figure 1a), but not ILC1 or ILC3, was significantly higher than that of CD45.1 wild-type (WT) cells (figure 1b). As the expression pattern of surface markers of ILC2s potentially varies [26], the expression of ILC2 markers on lineage^{-}CD45^{+} cells was compared using t-distributed stochastic neighbor embedding (t-SNE) [27, 28]. A cell cluster exhibiting high-expression levels of T1/ST2, Sca-1 and KLRG1 was identified among the 3 clusters obtained by the analysis (figure 1c), and the cluster is consistent with ILC2s we initially defined (figure 1a). Both WT and *Regnase-1*$^{-/-}$ cells were found in the cluster, though the numbers of *Regnase-1*$^{-/-}$ ILC2s were much more than the WT (figure 1d). The WT and *Regnase-1*$^{-/-}$ ILC2 clusters also express other markers for ILC2s such as c-kit and CD127 (IL-7R), whereas the expression levels of CD25 and Thy1.2 levels were decreased in *Regnase-1*$^{-/-}$ ILC2s (figure 1e). In addition to ILC2s, populations of effector/memory CD4^{+} T cells and Th2 cells (CD3^{+}CD4^{+}GATA3^{+} cells) were elevated with Regnase-1 deficiency, suggesting that Regnase-1 regulates the number of type 2 immune cells in a cell-intrinsic manner (figure 1b and supplementary figure S1B). When type 2 effector cells were examined, Regnase-1 deficiency increased the basophils, but not eosinophils or mast cells (figure 1b). Conversely, an increase of CD45.2 *Regnase-1*$^{-/-}$ ILC2 population in fat-associated lymphoid cells was not found compared with CD45.1 WT cells, indicating the tissue specific feature of ILC2s increase in the absence of Regnase-1 (supplementary figure S2).

The number of ILC2 was also increased in the lung of *Regnase-1*$^{-/-}$ mice (figure 1f).

When we generated mice lacking both Regnase-1 and Rag2, a significant increase in ILC2s was observed in the lung or BAL fluid in the absence of Regnase-1 indicating that the increase of *Regnase-1*-deficient ILC2s does not depend on the secondary effect of T cell activation (figure 1g). Next, the eosinophils in the lungs were examined, which are known to be elicited by ILC2s and Th2 cells. We found that eosinophils were highly increased in the lungs of *Regnase-1*$^{-/-}$ mice (figure 1h). The increased numbers of eosinophils in the lungs and the BAL of *Regnase-1*-deficient mice were observed even when the mice lacked T cells due to *Rag2* deficiency (figure 1i and supplementary figure S3), suggesting the critical role of *Regnase-1* in ILC2s for eosinophilic inflammation.

Regnase-1 regulates ILC2 proliferation and activation

We next examined if Regnase-1 controls ILC2 proliferation or cell death using the competitive transfer model. The expression of a proliferation marker Ki-67 was significantly higher in *Regnase-1*-deficient ILC2s compared with WT ILC2s (figure 2a). In contrast, there was no difference in the levels of a cell viability marker (figure 2b), indicating that Regnase-1 negatively regulates the cell proliferation, but not death, of ILC2s.

We then investigated whether this enhanced proliferation is recapitulated in ILC2s cultured *in vitro*. We sorted ILC2s from the lung of WT and *Regnase-1*$^{-/-}$ mice, then cultured them with IL-2 and IL-7, a culture condition inducing homeostatic expansion of ILC2s[26], Unexpectedly, both WT and *Regnase-1*$^{-/-}$ ILC2s proliferated to produce similar numbers of cells after 5 days of culture (figure 2c), suggesting that IL-2 and IL-7 are not sufficient to evoke enhanced proliferation induced under Regnase-1 deficiency *in vivo*.

To further characterize the effect of Regnase-1 deficiency in ILC2 activation, we evaluated ILC2-signature surface molecules on the ILC2s. Interestingly, the expression levels of ICOS and KLRG1 were significantly upregulated in *Regnase-1*-deficient ILC2s in the

competitive BM transfer model or in *Rag2*$^{-/-}$*Regnase-1*$^{-/-}$ mice (figure 2d and supplementary figure S4). ICOS stimulation promotes the proliferation of ILC2s by stabilizing STAT5 phosphorylation[29], and *Icos* mRNA is directly degraded by Regnase-1[5]. In contrast, it was shown that KLRG1 stimulation did not induce the proliferation of ILC2s[30]. Therefore, we hypothesized that Regnase-1 suppresses the proliferation of ILC2s through the downregulation of ICOS. To exclude the contamination of T cells which also express ICOS, we used *Rag2*$^{-/-}$ mice and *Rag2*$^{-/-}$*Regnase-1*$^{-/-}$ mice for the purification and culture of ILC2. Treatment with an ICOS-stimulating antibody significantly increased the number of cultured *Regnase-1*-deficient ILC2s compared with WT (figure 2e), accompanied by the augmentation of STAT5 phosphorylation (figure 2f). These data indicate that the Regnase-1-mediated ICOS downregulation contributes to the maintenance of ILC2 numbers in the lung. *Regnase-1*-deficient ILC2s were also found to show decreased expression of Thy1.2 (figure 2d), which suggested the activation of ILC2s[30, 31]. The secretion of ILC2-signature cytokines such as IL-5 and IL-13 as well as IL-6, which is the established target of Regnase-1, was elevated in cultured *Regnase-1*-deficient ILC2s (figure 2g). These data demonstrate that Regnase-1 is important not only for controlling the numbers of ILC2s but also for maintaining quiescent status of ILC2s in the steady state condition[30, 31]. Collectively, these data demonstrate that Regnase-1 is important not only for controlling the numbers of ILC2s but also for maintaining quiescent status of ILC2s.

Regnase-1-deficient ILC2s promote pulmonary fibrosis

We next investigated the relevance of Regnase-1 expressed in ILC2s in pulmonary diseases. For this purpose, we simultaneously isolated WT and *Regnase-1*-deficient ILC2s from the lung of competitively transferred mice, and performed transcriptome analysis. We found 289 differentially expressed genes (DEGs) between WT and *Regnase-1*-deficient ILC2s. Among

them, 221 genes showed increased expression in *Regnase-1*-deficient ILC2s compared with WT ILC2s (hereafter "upregulated genes") (figure 3a and supplementary table S3 and S4). The upregulated genes included cytokines such as *Il4*, *Il5*, *Il6* and *Il13* (figure 3b). We then analyzed the associations between the upregulated genes and pulmonary diseases by using Comparative Toxicogenomics Database (CTD)[32]. Consistent with the activation of ILC2s, genes categorized to "Asthma"[33, 34] were significantly enriched (figure 3c and supplementary table S5). In addition, the genes categorized to "Pulmonary Fibrosis" were also highly enriched (figure 3c and supplementary table S5). Analysis with human orthologues of the upregulated genes reproduced the same set of diseases (supplementary figure S5A). While "Pulmonary Fibrosis" and "Asthma" related genes overlapped each other (supplementary table S6), "Pulmonary Fibrosis"-specific genes and overlapping genes were significantly more frequent compared with "Asthma"-specific genes (figure 3d), implying that Regnase-1 regulates "Pulmonary Fibrosis"-related genes more broadly than "Asthma"-related genes. These data suggest the association of Regnase-1 in ILC2s with pulmonary diseases especially fibrosis.

Therefore, the relationship between Regnase-1 in ILC2s and pulmonary fibrosis in mice was investigated. First, RT-qPCR analysis revealed that bleomycin treatment decreased *Regnase-1* expression in lung ILC2s, suggesting that Regnase-1 expression is decreased following the development of pulmonary fibrosis in mice (figure 3e). Then we intratracheally administered bleomycin in *Rag2*$^{-/-}$*Il2rc*$^{-/-}$ mice, which lack all mature T cells, B cells and ILCs, followed by the intratracheal transfer of cultured ILC2s derived from *Regnase-1*$^{-/-}$*Rag2*$^{-/-}$ or control (*Rag2*$^{-/-}$) mice[22] (supplementary method and supplementary figure S5B). Mice receiving *Regnase-1*-deficient ILC2s (KO-transfer) exhibited more severe fibrotic lesions compared with mice without ILC2 transfer (NO-transfer) or receiving the transfer of control ILC2s (WT-transfer) (figures 3f and g). In addition, collagen deposition in

the lung as well as the levels of IL-4 and IL-13, potent inducers of fibrosis[35], were elevated in the BAL fluid of mice receiving *Regnase-1*-deficient ILC2s (figure 3g, figure 3i and supplementary table S2). Collectively, these data indicate that Regnase-1 expressed in ILC2s is critical for the regulation of pulmonary fibrosis in mice.

Regnase-1 negatively regulates the expression of genes associated with pulmonary fibrosis

Since fibrosis-associated genes *Il4* and *Il13* are not directly degraded by Regnase-1, we hypothesized that Regnase-1 primarily regulates the transcriptional program(s) of ILC2s which subsequently control cytokines and fibrosis-associated genes. To identify the Regnase-1-regulated transcriptional programs, we employed two approaches. First was the analysis on the association between the upregulated genes and CGAP BioCarta Pathways[36, 37], which revealed a significant enrichment of the GATA3 pathway, which is critical for the regulation of IL-4, IL-5 and IL-13 (figure 4a)[38]. Intriguingly, *Gata3* mRNA levels were significantly increased in *Regnase-1*-deficient ILC2s (figure 4b), which is consistent with the previous report that *Gata3* mRNA is a direct target of Regnase-1[7]. As the second approach, we screened transcription factor binding sites of upregulated genes associated with "Pulmonary Fibrosis" in CTD (see supplementary methods), and isolated a set of transcription factors potentially regulating pulmonary fibrosis-associated genes (figure 4c and supplementary table S7). Among identified transcription factors, the expression of *Egr1*, *Nfkb1* and *Fos* was significantly increased in *Regnase-1*-deficient ILC2s (figure 4d and supplementary table S8). Especially, the expression level of *Egr1* was more than 60-times higher in *Regnase-1*-deficient ILC2s (figure 4d). A luciferase reporter harboring *Egr1* 3′ UTR was suppressed by the overexpression of WT, but not nuclease activity-inactivated mutant (D141N), Regnase-1 (figure 4e), indicating that the *Egr1* mRNA is directly degraded

by Regnase-1. Taken together, pro-fibrotic function of ILC2s in the lung is critically suppressed by Regnase-1 via the post-transcriptional regulation of transcriptional networks including GATA3 and EGR-1.

Regnase-1 expression levels negatively correlate with the ILC2 population in human BAL

These results prompted us to investigate the clinical significance of Regnase-1-mediated regulation of ILC2s in IPF patients. Human ILC2s were defined as $CD45^{+}lineage^{-}CD127^{+}CRTH2^{+}CD161^{+}$ cells (supplementary figure S6). We analyzed Regnase-1 expression levels in BAL ILC2s from IPF patients and control subjects by newly generating a flow cytometry-based method of intracellular Regnase-1 staining (supplementary method, supplementary figure S7A-C and supplementary table S9). Interestingly, a significant negative association was found between Regnase-1 expression levels and the population as well as the number of ILC2s in BAL (figure 5a and supplementary figure S8), suggesting that Regnase-1 regulates ILC2 numbers in the lungs both in mouse and human. However, Regnase-1 expression levels or ILC2 populations were not significantly different between IPF patients and controls (figure 5b and c). Whether BAL ILC2 populations were associated with the clinical course among IPF patients was then investigated. We found that ILC2 populations in BAL tend to be increased in IPF patients who exhibited complications with disease progression within 1 year, although the difference did not reach statistical significance (figure 5d).

High number of peripheral blood ILC2s predicts poor prognosis in IPF patients

Although ILC2s are considered tissue resident, the number of ILC2s in the peripheral blood is suggested to correlate with the local inflammatory conditions contributing the increase in

ILC2[34, 39]. Therefore, to increase the number of patients, we quantified the number of ILC2s in the peripheral blood of IPF patients and analyzed the association between the clinical indices. We found that ICOS expression levels were positively associated with the number of blood ILC2s in IPF patients (figure 6a). However, no statistically significant correlations were found between peripheral blood ILC2 numbers and pulmonary function indices (figure 6b). Also, no correlations were observed between the ILC2 numbers and plasma levels of IL-4, IL-5 and IL-13 (supplementary figure S9A). These results suggest that the peripheral blood ILC2s do not reflect the intensity of systemic type 2 inflammation among IPF patients.

We next analyzed the associations between peripheral blood ILC2s and the survival of IPF. Based on a receiver operating characteristic curve to identify respiratory death (supplementary figure S9B), we divided patients into two groups according to a peripheral blood ILC2 number of 1500 cells/ml. Patients with ILC2s $\geq$ 1500 cells/ml showed lower %FVC, but otherwise the two groups showed no significant differences (table 1). Notably, patients with peripheral blood ILC2s $\geq$ 1500 cells/ml showed strikingly worse respiratory mortality and all-cause mortality (figure 6c). The three-year survival rates of the patients with the higher and lower ILC2 numbers were 0.239 and 0.734, respectively. By setting these values, the power of analysis was calculated as 0.891. Death due to chronic respiratory failure was significantly common among the patients with peripheral blood ILC2s $\geq$ 1500 cells/ml (supplementary table S10). These data suggest that higher ILC2 numbers in the blood are associated with the disease severity and poor prognosis.

To further investigate whether ILC2s could predict prognosis independent of other confounding factors, we performed univariate and multivariate analyses for respiratory mortality. In univariate analysis, ILC2s $\geq$ 1500 cells/ml, %FVC, %predicted diffusion lung capacity of carbon monoxide (%DLco) and the lowest saturation of peripheral O_2 (SpO_2)

value in the 6-minute-walk test (6MWT) were significantly associated with the respiratory mortality. On the other hand, multivariate analysis revealed that the peripheral blood ILC2 number $\geq$ 1500 cells/ml was the independent factor for respiratory mortality, while other factors except the lowest SpO_2 value in the 6MWT failed to remain as significant factors (table 2). These data suggest that an increase in the number of peripheral blood ILC2s can correlate with IPF disease severity, and is an independent and strong predictive factor for survival (supplementary figure S10).

Discussion

In this study, we discovered that Regnase-1 is critical for the regulation of proliferation and activation of ILC2s, and inhibition of pulmonary fibrosis progression. Compared with the roles of ILC2s in allergic diseases such as bronchial asthma, a small number of studies have focused on their significance in pulmonary fibrosis, and the regulatory mechanisms for pro-fibrotic functions is largely unknown[40]. In this regard, mice lacking Regnase-1 is a novel mouse model for the functional analysis of ILC2s in suppressing pulmonary fibrosis.

Although Regnase-1 degrades a set of cytokine genes, such as *Il6*, *Il12b* and *Il2* in macrophages and T cells, it fails to recognize *Il4* and *Il13* genes[5], which are abundantly produced by ILC2s. Instead, Regnase-1 seems to regulate these cytokines via suppression of transcription factors such as *Gata3* and *Egr1*. It has been shown that increased GATA3 expression promoted the production of IL-4, IL-5 and IL-13 in ILC2s[38]. These cytokine genes were included in the categories of both pulmonary fibrosis- and asthma-associated genes in CTD, suggesting that increased GATA3 expression contributes to the development of both diseases[35]. A very recent paper reported that Regnase-1 degradation in ILC2 through IL-25 or IL-33 stimulation enhanced papain-induced respiratory tract inflammation, which indicates the relationship between Regnase-1 in ILC2s and asthma [41]. On the other hand, Donovan et al. reported that exposure of *Rora*$^{fl/fl}$ *Il7r*^{Cre} mice, which lack ILC2s, to cigarette smoking showed increased *Il13* expression and collagen deposition, though they are protected from emphysema [42]. Thus, the functions of ILC2s in the lungs may be different depending on the disease models, though further studies are required to uncover the precise mechanisms how ILC2s contribute to these lung diseases.

In addition to GATA3, we discovered that Regnase-1 profoundly suppressed *Egr1* mRNA expression via the 3′ UTR. Previous studies showed that EGR-1 enhances the transcription of various fibrosis-associated genes such as *Tgfb1*[43, 44]. Indeed, we found

that the mRNA levels of *Tgfb1* in Regnase1-deficient ILC2s were much higher than WT ILC2s, although they failed to show statistical significance owing to the large deviation (Supplementary table S3). Thus, it is plausible that Regnase-1 regulates the pro-fibrotic function of ILC2s by modifying transcriptional networks including GATA3 and EGR-1, though further studies are required to uncover the entire transcriptional and post-transcriptional gene expression networks that control pulmonary fibrosis via ILC2s.

We found that Regnase-1 regulates the number of lung ILC2s in a cell-intrinsic manner in mice by controlling the ICOS expression. While ICOSL was shown to be expressed on myeloid cells such as the dendritic cells and macrophages or ILC2s [29] [45], this study found that ICOSL expression on ILC2s was much lower than the myeloid cells in the lungs (data not shown). Therefore, ILC2 proliferation likely requires additional ICOS stimulation via cells expressing ICOSL or the supplementation of ICOS-stimulating antibody even in the absence of Regnase-1. On the other hand, ICOS-stimulating antibody did not enhance the proliferation of WT ILC2s. We speculate that Regnase-1 controls the threshold of responses to ICOS stimulation in ILC2s by suppressing the expression of ICOS and its signaling molecules, though further studies are required to elucidate the detailed mechanism.

Furthermore, the ILC2 population in human BAL was negatively correlated with Regnase-1 expression levels, suggesting that Regnase-1-mediated regulation of the ILC2 number in the lung is shared between mice and humans. Considering that ILC2s could promote fibrosis and that a high number of ILC2s was associated with poor prognosis among IPF patients, it is suggested that an inadequate activation and proliferation of ILC2s accelerates the progression of IPF. We also discovered that ICOS expression on the surface of blood ILC2s was positively correlated with the number of ILC2s, which evokes us the speculation that enhanced ICOS signaling contributes to an increased number of ILC2s in IPF patients. Because Regnase-1 restricts ILC2 proliferation potentially through suppressing

ICOS expression via the 3′ UTR[5], the Regnase1–ICOS axis might play a role in the regulation of blood ILC2s in IPF patients. In addition, Regnase-1 can critically restrict the pro-fibrotic function of ILC2s, therefore the stabilization of Regnase-1 in ILC2s may have a therapeutic property. In future studies, it is expected that an interventional method to induce Regnase-1 expression *in vivo* will be established and its efficacy in protection against pulmonary fibrosis will be evaluated.

The limitation of this study is that the number of clinical samples available was quite small, which reduced the validity of the clinical data in this study. Especially, it is desired to validate the cutoff value of peripheral blood ILC2 number for the prediction of prognosis among IPF patients by using an independent cohort. To overcome this limitation, conducting prospective studies with larger number of cases are expected to be done to elucidate the clinical significance of Regnase-1 and ILC2s in IPF.

Despite these limitations, this study showed for the first time that Regnase-1 regulates the proliferation and profibrotic function of ILC2s in the lungs, and an increase in the number of ILC2s in the blood was associated with poor survival, suggesting that Regnase-1 is a critical posttranscriptional regulator of the profibrotic function of ILC2s both in mouse and human. Further studies are required to confirm the clinical significance of ILC2s in IPF with a larger cohort and to evaluate the therapeutic potential of Regnase-1 stabilization for ILC2s.

Acknowledgments

We thank all members of our laboratory for discussions. We also thank Natsuko Otaki (Laboratory for Innate Immune Systems, RIKEN Center for Integrative Medical Sciences), Hisako Matsumoto, Atsuyasu Sato, Shinpei Goto and Kiyoshi Uemasu (Department of Respiratory Medicine, Graduate School of Medicine, Kyoto University, Kyoto, Japan) for discussions and kind instructions. We are also grateful for Kazuko Uno (Louis Pasteur Center for Medical Research, Kyoto, Japan) for performing multiplex analysis, and Tomoko Nakanishi, Takashi Niwamoto, Naoya Ikegami, Yuko Murase, Kohei Ikezoe, and Akihiko Sokai (Department of Respiratory Medicine, Graduate School of Medicine, Kyoto University, Kyoto, Japan) for collecting clinical data and samples. The authors would like to thank Enago (www.enago.jp) for the English language review.

Author contributions: Y.N. and O.T. developed the study concept and design. Y.N. performed the majority of experiments, clinical data collection and analysis of data. A.Y., Y.H. and Y.M. also developed experimental design and performed experiments. M.Y., T.U., T.M. helped with the experiments. A.V. and Y.S. performed data analysis. A.S. and T.T. performed histological analysis. T.Handa. supervised clinical study. K.T., K.W., T.Hirai. and K.C. performed clinical data collection and helped with clinical data analysis. K.M. helped with the development of study concept and experimental design, and provided critical materials. N.Y. H.T. and O.T. wrote the manuscript. O.T. led the whole project.

Conflict of interests: The Department of Respiratory Care and Sleep Control Medicine (Y.N. and K.C.) is funded by endowments from Philips-Respironics, ResMed, Fukuda Denshi and Fukuda Lifetec-Keiji to Kyoto University. Otherwise the authors have declared that no conflict of interest no conflict of interest exists.

Support statement: This research was supported by a Grant-in-Aid for Scientific Research (S) (18H05278, to O.T.), Grant-in-Aid for Scientific Research (C) (26461187, to T.H.),

Grant-in-Aid from the Japan Society for the Promotion of Science Grant-in-Aid for Research Activity start-up (18H06221, to Y.N.), and Grant-in-Aid for Scientific Research on Innovative Areas ‘Genome Science’ (221S0002, 16H06279 to T.M.). This research was also supported by AMED under Grant Number JP19gm4010002 (to O.T.).

References

1. Iwasaki A, Foxman EF, Molony RD. Early local immune defences in the respiratory tract. *Nat Rev Immunol* 2017: 17(1): 7-20.

2. Carpenter S, Ricci EP, Mercier BC, Moore MJ, Fitzgerald KA. Post-transcriptional regulation of gene expression in innate immunity. *Nature Reviews Immunology* 2014: 14: 361.

3. Mino T, Takeuchi O. Post-transcriptional regulation of immune responses by RNA binding proteins. *Proc Jpn Acad Ser B Phys Biol Sci* 2018: 94(6): 248-258.

4. Matsushita K, Takeuchi O, Standley DM, Kumagai Y, Kawagoe T, Miyake T, Satoh T, Kato H, Tsujimura T, Nakamura H, Akira S. Zc3h12a is an RNase essential for controlling immune responses by regulating mRNA decay. *Nature* 2009: 458(7242): 1185-1190.

5. Uehata T, Iwasaki H, Vandenbon A, Matsushita K, Hernandez-Cuellar E, Kuniyoshi K, Satoh T, Mino T, Suzuki Y, Standley DM, Tsujimura T, Rakugi H, Isaka Y, Takeuchi O, Akira S. Malt1-induced cleavage of regnase-1 in CD4(+) helper T cells regulates immune activation. *Cell* 2013: 153(5): 1036-1049.

6. Mino T, Murakawa Y, Fukao A, Vandenbon A, Wessels HH, Ori D, Uehata T, Tartey S, Akira S, Suzuki Y, Vinuesa CG, Ohler U, Standley DM, Landthaler M, Fujiwara T, Takeuchi O. Regnase-1 and Roquin Regulate a Common Element in Inflammatory mRNAs by Spatiotemporally Distinct Mechanisms. *Cell* 2015: 161(5): 1058-1073.

7. Peng H, Ning H, Wang Q, Lu W, Chang Y, Wang TT, Lai J, Kolattukudy PE, Hou R, Hoft DF, Dykewicz MS, Liu J. Monocyte chemotactic protein-induced protein 1 controls allergic airway inflammation by suppressing IL-5-producing TH2 cells through the Notch/Gata3 pathway. *J Allergy Clin Immunol* 2018: 142(2): 582-594 e510.

8. Nakatsuka Y, Vandenbon A, Mino T, Yoshinaga M, Uehata T, Cui X, Sato A, Tsujimura T, Suzuki Y, Sato A, Handa T, Chin K, Sawa T, Hirai T, Takeuchi O. Pulmonary

Regnase-1 orchestrates the interplay of epithelium and adaptive immune systems to protect against pneumonia. *Mucosal Immunol* 2018: 11(4): 1203-1218.

9. Monin L, Gudjonsson JE, Childs EE, Amatya N, Xing X, Verma AH, Coleman BM, Garg AV, Killeen M, Mathers A, Ward NL, Gaffen SL. MCPIP1/Regnase-1 Restricts IL-17A- and IL-17C-Dependent Skin Inflammation. *J Immunol* 2017: 198(2): 767-775.

10. Wei J, Long L, Zheng W, Dhungana Y, Lim SA, Guy C, Wang Y, Wang YD, Qian C, Xu B, Kc A, Saravia J, Huang H, Yu J, Doench JG, Geiger TL, Chi H. Targeting REGNASE-1 programs long-lived effector T cells for cancer therapy. *Nature* 2019: 576(7787): 471-476.

11. Richeldi L, Varone F, Bergna M, de Andrade J, Falk J, Hallowell R, Jouneau S, Kondoh Y, Morrow L, Randerath W, Strek M, Tabaj G. Pharmacological management of progressive-fibrosing interstitial lung diseases: a review of the current evidence. *Eur Respir Rev* 2018: 27(150).

12. Wynn TA, Ramalingam TR. Mechanisms of fibrosis: therapeutic translation for fibrotic disease. *Nat Med* 2012: 18(7): 1028-1040.

13. Magnini D, Montemurro G, Iovene B, Tagliaboschi L, Gerardi RE, Lo Greco E, Bruni T, Fabbrizzi A, Lombardi F, Richeldi L. Idiopathic Pulmonary Fibrosis: Molecular Endotypes of Fibrosis Stratifying Existing and Emerging Therapies. *Respiration* 2017: 93(6): 379-395.

14. Moro K, Yamada T, Tanabe M, Takeuchi T, Ikawa T, Kawamoto H, Furusawa J, Ohtani M, Fujii H, Koyasu S. Innate production of T(H)2 cytokines by adipose tissue-associated c-Kit(+)Sca-1(+) lymphoid cells. *Nature* 2010: 463(7280): 540-544.

15. Price AE, Liang HE, Sullivan BM, Reinhardt RL, Eisley CJ, Erle DJ, Locksley RM. Systemically dispersed innate IL-13-expressing cells in type 2 immunity. *Proc Natl Acad Sci U S A* 2010: 107(25): 11489-11494.

16. Dahlgren MW, Molofsky AB. All along the watchtower: group 2 innate lymphoid

cells in allergic responses. *Curr Opin Immunol* 2018: 54: 13-19.

17. Starkey MR, McKenzie AN, Belz GT, Hansbro PM. Pulmonary group 2 innate lymphoid cells: surprises and challenges. *Mucosal Immunol* 2019: 12(2): 299-311.

18. Hams E, Armstrong ME, Barlow JL, Saunders SP, Schwartz C, Cooke G, Fahy RJ, Crotty TB, Hirani N, Flynn RJ, Voehringer D, McKenzie AN, Donnelly SC, Fallon PG. IL-25 and type 2 innate lymphoid cells induce pulmonary fibrosis. *Proc Natl Acad Sci U S A* 2014: 111(1): 367-372.

19. Li D, Guabiraba R, Besnard AG, Komai-Koma M, Jabir MS, Zhang L, Graham GJ, Kurowska-Stolarska M, Liew FY, McSharry C, Xu D. IL-33 promotes ST2-dependent lung fibrosis by the induction of alternatively activated macrophages and innate lymphoid cells in mice. *J Allergy Clin Immunol* 2014: 134(6): 1422-1432 e1411.

20. Kindermann M, Knipfer L, Atreya I, Wirtz S. ILC2s in infectious diseases and organ-specific fibrosis. *Semin Immunopathol* 2018: 40(4): 379-392.

21. Cao X, Shores EW, Hu-Li J, Anver MR, Kelsall BL, Russell SM, Drago J, Noguchi M, Grinberg A, Bloom ET, et al. Defective lymphoid development in mice lacking expression of the common cytokine receptor gamma chain. *Immunity* 1995: 2(3): 223-238.

22. Yang Q, Ge MQ, Kokalari B, Redai IG, Wang X, Kemeny DM, Bhandoola A, Haczku A. Group 2 innate lymphoid cells mediate ozone-induced airway inflammation and hyperresponsiveness in mice. *J Allergy Clin Immunol* 2016: 137(2): 571-578.

23. Cui X, Mino T, Yoshinaga M, Nakatsuka Y, Hia F, Yamasoba D, Tsujimura T, Tomonaga K, Suzuki Y, Uehata T, Takeuchi O. Regnase-1 and Roquin Nonredundantly Regulate Th1 Differentiation Causing Cardiac Inflammation and Fibrosis. *J Immunol* 2017: 199(12): 4066-4077.

24. Raghu G, Rochwerg B, Zhang Y, Garcia CA, Azuma A, Behr J, Brozek JL, Collard HR, Cunningham W, Homma S, Johkoh T, Martinez FJ, Myers J, Protzko SL, Richeldi L,

Rind D, Selman M, Theodore A, Wells AU, Hoogsteden H, Schunemann HJ, American Thoracic S, European Respiratory s, Japanese Respiratory S, Latin American Thoracic A. An Official ATS/ERS/JRS/ALAT Clinical Practice Guideline: Treatment of Idiopathic Pulmonary Fibrosis. An Update of the 2011 Clinical Practice Guideline. *Am J Respir Crit Care Med* 2015: 192(2): e3-19.

25. Raghu G, Remy-Jardin M, Myers JL, Richeldi L, Ryerson CJ, Lederer DJ, Behr J, Cottin V, Danoff SK, Morell F, Flaherty KR, Wells A, Martinez FJ, Azuma A, Bice TJ, Bouros D, Brown KK, Collard HR, Duggal A, Galvin L, Inoue Y, Jenkins RG, Johkoh T, Kazerooni EA, Kitaichi M, Knight SL, Mansour G, Nicholson AG, Pipavath SNJ, Buendia-Roldan I, Selman M, Travis WD, Walsh S, Wilson KC. Diagnosis of Idiopathic Pulmonary Fibrosis. An Official ATS/ERS/JRS/ALAT Clinical Practice Guideline. *Am J Respir Crit Care Med* 2018: 198(5): e44-e68.

26. Moro K, Ealey KN, Kabata H, Koyasu S. Isolation and analysis of group 2 innate lymphoid cells in mice. *Nat Protoc* 2015: 10(5): 792-806.

27. Cameron GJM, Cautivo KM, Loering S, Jiang SH, Deshpande AV, Foster PS, McKenzie ANJ, Molofsky AB, Hansbro PM, Starkey MR. Group 2 Innate Lymphoid Cells Are Redundant in Experimental Renal Ischemia-Reperfusion Injury. *Front Immunol* 2019: 10(826).

28. Van Gassen S, Callebaut B, Van Helden MJ, Lambrecht BN, Demeester P, Dhaene T, Saeys Y. FlowSOM: Using self-organizing maps for visualization and interpretation of cytometry data. *Cytometry A* 2015: 87(7): 636-645.

29. Maazi H, Patel N, Sankaranarayanan I, Suzuki Y, Rigas D, Soroosh P, Freeman GJ, Sharpe AH, Akbari O. ICOS:ICOS-ligand interaction is required for type 2 innate lymphoid cell function, homeostasis, and induction of airway hyperreactivity. *Immunity* 2015: 42(3): 538-551.

30. Huang Y, Guo L, Qiu J, Chen X, Hu-Li J, Siebenlist U, Williamson PR, Urban JF, Jr., Paul WE. IL-25-responsive, lineage-negative KLRG1(hi) cells are multipotential 'inflammatory' type 2 innate lymphoid cells. *Nat Immunol* 2015: 16(2): 161-169.

31. Miyamoto C, Kojo S, Yamashita M, Moro K, Lacaud G, Shiroguchi K, Taniuchi I, Ebihara T. Runx/Cbfbeta complexes protect group 2 innate lymphoid cells from exhausted-like hyporesponsiveness during allergic airway inflammation. *Nat Commun* 2019: 10(1): 447.

32. Davis AP, Grondin CJ, Johnson RJ, Sciaky D, McMorran R, Wiegers J, Wiegers TC, Mattingly CJ. The Comparative Toxicogenomics Database: update 2019. *Nucleic Acids Res* 2019: 47(D1): D948-d954.

33. Scanlon ST, McKenzie AN. Type 2 innate lymphoid cells: new players in asthma and allergy. *Curr Opin Immunol* 2012: 24(6): 707-712.

34. Bartemes KR, Kephart GM, Fox SJ, Kita H. Enhanced innate type 2 immune response in peripheral blood from patients with asthma. *J Allergy Clin Immunol* 2014: 134(3): 671-678 e674.

35. Gieseck RL, 3rd, Wilson MS, Wynn TA. Type 2 immunity in tissue repair and fibrosis. *Nat Rev Immunol* 2018: 18(1): 62-76.

36. Huang da W, Sherman BT, Lempicki RA. Systematic and integrative analysis of large gene lists using DAVID bioinformatics resources. *Nat Protoc* 2009: 4(1): 44-57.

37. Huang da W, Sherman BT, Lempicki RA. Bioinformatics enrichment tools: paths toward the comprehensive functional analysis of large gene lists. *Nucleic Acids Res* 2009: 37(1): 1-13.

38. Klein Wolterink RG, Serafini N, van Nimwegen M, Vosshenrich CA, de Bruijn MJ, Fonseca Pereira D, Veiga Fernandes H, Hendriks RW, Di Santo JP. Essential, dose-dependent role for the transcription factor Gata3 in the development of IL-5+ and IL-13+ type 2 innate

lymphoid cells. *Proc Natl Acad Sci U S A* 2013: 110(25): 10240-10245.

39. Omata Y, Frech M, Primbs T, Lucas S, Andreev D, Scholtysek C, Sarter K, Kindermann M, Yeremenko N, Baeten DL, Andreas N, Kamradt T, Bozec A, Ramming A, Kronke G, Wirtz S, Schett G, Zaiss MM. Group 2 Innate Lymphoid Cells Attenuate Inflammatory Arthritis and Protect from Bone Destruction in Mice. *Cell Rep* 2018: 24(1): 169-180.

40. Klose CS, Artis D. Innate lymphoid cells as regulators of immunity, inflammation and tissue homeostasis. *Nat Immunol* 2016: 17(7): 765-774.

41. Matsushita K, Tanaka H, Yasuda K, Adachi T, Fukuoka A, Akasaki S, Koida A, Kuroda E, Akira S, Yoshimoto T. Regnase-1 degradation is crucial for IL-33- and IL-25-mediated ILC2 activation. *JCI Insight* 2020: 5(4).

42. Donovan C, Starkey MR, Kim RY, Rana BMJ, Barlow JL, Jones B, Haw TJ, Mono Nair P, Budden K, Cameron GJM, Horvat JC, Wark PA, Foster PS, McKenzie ANJ, Hansbro PM. Roles for T/B lymphocytes and ILC2s in experimental chronic obstructive pulmonary disease. *J Leukoc Biol* 2019: 105(1): 143-150.

43. Liu C, Adamson E, Mercola D. Transcription factor EGR-1 suppresses the growth and transformation of human HT-1080 fibrosarcoma cells by induction of transforming growth factor beta 1. *Proc Natl Acad Sci U S A* 1996: 93(21): 11831-11836.

44. Liu C, Calogero A, Ragona G, Adamson E, Mercola D. EGR-1, the reluctant suppression factor: EGR-1 is known to function in the regulation of growth, differentiation, and also has significant tumor suppressor activity and a mechanism involving the induction of TGF-beta1 is postulated to account for this suppressor activity. *Crit Rev Oncog* 1996: 7(1-2): 101-125.

45. Marinelli O, Nabissi M, Morelli MB, Torquati L, Amantini C, Santoni G. ICOS-L as a Potential Therapeutic Target for Cancer Immunotherapy. *Curr Protein Pept Sci* 2018: 19(11):

1107-1113.

Table 1. Background of cases in the analysis of ILC2s in peripheral blood

	ILC2 ≦1500 (n = 37)	ILC2 > 1500 (n = 11)	*P*-value
Male sex, n	33 (89.2)	9 (81.8)	0.609
Age, years	73.00 [69.00, 79.00]	71.00 [67.50, 75.50]	0.350
Never smoker, n	3 (8.3)	0 (0.0)	>0.99
Brinkman index	740.00 [460.00, 1055.00]	900.00 [655.00, 1840.00]	0.175
Diabetes Mellitus, n	11 (29.7)	4 (36.4)	0.720
Bronchial Asthma, n	4 (10.8)	1 (9.1)	>0.99
Pirfenidone usage, n	6 (16.2)	5 (45.5)	0.095
Corticosteroid usage, n	3 (8.1)	1 (9.1)	>0.99
PaO_2, mmHg	82.80 [74.90, 93.70]	77.80 [68.85, 80.20]	0.128
$PaCO_2$,mmHg	39.10 [36.30, 40.40]	41.40 [38.20, 42.60]	0.113
%FVC, %	87.90 [82.40, 105.30]	72.90 [63.10, 87.20]	0.010
%DLco, %	43.30 [34.20, 53.20]	42.00 [36.40, 47.43]	0.594
$\%FEV_1$, %	90.20 [82.20, 103.40]	77.90 [66.75, 92.80]	0.032
FEV_1/FVC, %	81.19 [77.39, 85.21]	83.57 [78.26, 86.72]	0.454
Composite Physiologic Index	46.41 [34.93, 55.64]	50.98 [43.31, 61.05]	0.138
6MWT distance, m	479.00 [412.00, 532.00]	420.00 [357.50, 469.50]	0.116
Lowest SpO_2 in 6MWT, %	86.50 [82.75, 90.00]	88.00 [77.50, 91.00]	0.548
SP-D, ng/ml	213.00 [108.00, 353.00]	285.00 [242.00, 479.00]	0.031
KL-6, U/ml	726.00 [621.00, 1190.00]	986.00 [472.00, 1535.00]	0.787
Death, n	12 (32.4)	6 (54.5)	0.288
Respiratory death, n	9 (24.3)	6 (54.5)	0.095

FVC: forced vital capacity, DLco: diffusion lung capacity of carbon monoxide,
FEV_1: forced expiratory volume in one second
6MWT: 6-minute walk test. SpO_2: saturation of peripheral O_2
PaO_2: partial pressure of O_2, $PaCO_2$: partial pressure of CO_2
Data are shown as number (%) or median [lower, higher interquartile range].
Fisher's exact test and Mann-Whitney U-test were used for analyses

Table 2. Univariate and multivariate analysis for respiratory mortality

Factor	Hazard ratio (95%CI)	*P*-value
Univariate analysis		
ILC2 > 1500 cells/ml	4.21 (1.45 – 12.19)	0.008
Age	1.00 (0.92 – 1.08)	0.938
Male sex	0.44 (0.12 – 1.57)	0.206
Corticosteroid usage	2.38 (0.67 – 8.46)	0.182
%FVC	0.95 (0.92 – 0.99)	0.006
%DLco	0.91 (0.86 – 0.97)	0.002
PaO_2	0.97 (0.93 – 1.00)	0.062
Brinkman index	1.00 (0.99 – 1.00)	0.484
6MWT SpO_2 minimum	0.88 (0.82 – 0.94)	< 0.0001
Multivariate analysis (Stepwise)		
ILC2 > 1500 cells/ml	7.17 (1.66 - 30.97)	0.008
Brinkman index	1.00 (0.99 - 1.00)	0.082
PaO_2	1.06 (0.98-1.13)	0.130
6MWT SpO_2 minimum	0.74 (0.62-0.88)	0.0008

FVC: forced vital capacity, DLco: diffusion lung capacity of carbon monoxide,
SpO_2: saturation of peripheral O_2, PaO_2: partial pressure of O_2
95%CI: 95% confidence interval, 6MWT: 6-minute walk test.
Cox proportional hazards test was used for the analyses

Figure legends

Figure 1. Regnase-1 negatively regulates the proliferation of ILC2 in a cell-intrinsic manner

(a) Representative figure for gating of ILC2s by flow cytometry. The identification of ILC2s in the lung of mice was done with $CD45^+Lineage^-T1/ST2^+KLRG^+Sca\text{-}1^+$ cells. Doublet depletion was done by the analysis of FSC-A/FSC-H and SSC-A/SSC-H. (**b**) Ratio of a $CD45.1^+$ (WT mice derived) and $CD45.2^+$ (*Regnase-1*$^{-/-}$ mice derived) population among each of cell type (n = 3-5). Data are the integrated numbers of two independent experiments. **(c)** A t-SNE analysis and subsequent clustering of $CD45^+Linage^-Ghost\text{-}dye^-$ cells in the lung following competitive BM transfer. The encircled population corresponds with ILC2. **(d)** Comparison of $CD45.1^+$ (WT mice-derived, blue) and $CD45.2^+$ (*Regnase-1*$^{-/-}$ mice-derived, red) $CD45^+Linage^-Ghost\text{-}dye^-$ cells by t-SNE analysis. The encircled population corresponds with ILC2. **(e)** Histograms of expression of c-Kit, CD127, CD25 and Thy1.2 on WT and *Regnase-1*$^{-/-}$ ILC2s. **(f, h)** Total number of ILC2s **(f)** or eosinophils **(h)** in the lung of WT mice (n = 4) and *Regnase-1*$^{-/-}$ mice (n = 3). Data are the representative of two independent experiments. **(g, i)** Comparison for the total number of ILC2s **(g)** or eosinophils **(i)** in the lung (left panel, n = 5) and BAL (right panel, n = 4) in the lung of *Rag2*$^{-/-}$ mice and *Regnase-1*$^{-/-}$*Rag2*$^{-/-}$ mice. Data are representative of two independent experiments. Data are shown as mean ± SD. Student's t-test was used for analyses.

Figure 2. *Regnase-1*-deficient ILC2s exhibit spontaneous activation

(a, b) Ratio of the $Ki67^+$ population **(a)** and viability marker (Ghost-dye) **(b)** among WT ($CD45.1^+$) and *Regnase-1*-deficient ILC2s ($CD45.2^+$) from the lung of competitively transferred mice (n = 6, the integrated numbers of two independent experiments). Data are shown as mean ± SD. Student's t-test was used for analyses.**(c)** *Ex-vivo* cell proliferation of

ILC2s isolated from the lung of WT or *Regnase-1*$^{-/-}$ mice cultured with 10 ng/ml recombinant mouse IL-2 plus IL-7 (n = 4). On day 1, 5000 cells were seeded and stimulated, and on day 5 the numbers of cells were evaluated. Data are representative of two independent experiments. **(d)** Cell surface expression levels of the indicated proteins among WT (CD45.1^{+}) and *Regnase-1*-deficient (CD45.2^{+}) ILC2s from the lung of competitively transferred mice. Expression levels were evaluated by flow cytometry. Data are representative of three independent experiments. **(e, f)** *Ex vivo* cell proliferation **(e)** and phospho-STAT5 protein levels evaluated by flow cytometry **(f)** of ILC2s isolated from the lung of *Rag2*$^{-/-}$ or *Regnase-1*$^{-/-}$*Rag2*$^{-/-}$ mice cultured with 10 ng/ml recombinant mouse IL-2 plus IL-7 supplemented with or without 3 μg/ml anti-ICOS stimulating antibody (n = 4). On day 1, 5000 cells were seeded and stimulated. On day 5, the number of cells and phospho-STAT5 expression levels were evaluated. Data are representative of two independent experiments. **(g)** Concentrations of indicated cytokines in the culture supernatant of ILC2s from the lungs of WT or *Regnase-1*$^{-/-}$ mice. In total, 5000 cells were suspended with 200 μl of medium supplemented with 10 ng/ml recombinant mouse IL-2 and IL-7, cultured and samples were collected on day 5. The concentrations were measured by Bioplex. MFI: mean fluorescence intensity.

Figure 3. *Regnase-1*-deficient ILC2s promote pulmonary fibrosis

(a) Volcano plot comparing the mRNA levels in WT (CD45.1^{+}) and *Regnase-1*-deficient (CD45.2^{+}) cells among ILC2s in the lung of competitive BM transfer model mice (n = 2). Expression levels in CD45.1^{+} cells were regarded as the control, and differentially expressed genes (DEGs) were defined as genes with FDR-*P*-values of < 0.05 and fold changes of < 0.5 or > 2.0, and highlighted. **(b)** Upregulated genes coding cytokines. FDR-*P*-values and fold-changes (expression levels in Regnase-1-deficient ILC2s compared with WT ILC2s)

were calculated by edgeR. **(c)** Top 15 human diseases that are associated with the upregulated genes. The Comparative Toxicogenomics Database (CTD) analyzer was used for the analysis. **(d)** Ratio of upregulated genes within "Pulmonary Fibrosis" but not in "Asthma" (categorized as Fibrosis only), within "Asthma" but not in "Pulmonary Fibrosis" (Asthma only) or both of "Pulmonary Fibrosis" and "Asthma" (Fibrosis & Asthma). Fisher's exact test was used for the analysis, and Bonferroni's adjustment was performed for multiple comparisons. (**e**) Quantitative PCR analysis for the expression levels of *Regnase-1* for ILC2s in the lungs of intratracheal bleomycin-treated *Rag2*$^{-/-}$ mice. *Rag2*$^{-/-}$ mice without bleomycin treatment were used as controls (n = 4). Data are shown as mean ± SD. **(f and g)** Histological images (f) and pathological lung fibrosis scores (g) of the bleomycin-induced pulmonary fibrosis model mice without cell transfer (No transfer, n = 5) or transferred with ILC2s derived from *Rag2*$^{-/-}$ or *Regnase-1*$^{-/-}$*Rag2*$^{-/-}$ mice (WT-transfer, n = 5 and KO-transfer, n = 8, respectively). Representative images with Hematoxylin and Eosin staining (H&E, upper) and Azan staining (lower) are shown in **(g)**. Data are the cumulative of three independent experiments. **(h)** Amount of collagen deposition measured with hydroxyproline assay (n = 7 for WT-transfer, n = 8 for KO-transfer). Data are the cumulative of three independent experiments. **(i)** Concentrations of indicated cytokines in the BAL fluid of WT-transfer and KO-transfer mice. The concentrations were measured by Bioplex.

Fisher's exact test and Student's t-test were used for the statistical analyses. For the adjustment of multiple comparisons, Holm's method was used.

Figure 4. Loss of Regnase-1 induces the expression of genes associated with pulmonary fibrosis

(a) Significantly enriched pathways for DEGs in the BioCarta Pathway. A *P*-value < 0.05 was regarded as significant. The analysis was done using DAVID 6.8 Bioinformatics

Resources. **(b)** Comparisons for RPKM values of *Gata3* between WT ($CD45.1^+$) and Regnase-1-deficient ($CD45.2^+$) cells. *P*-values (FDR-*P*-values) were calculated by edgeR. **(c)** Enriched transcription factor binding motifs associated with the upregulated genes categorized in "Pulmonary Fibrosis" in the Comparative Toxicogenomics Database. Screening was performed based on the JASPAR and TRANSFAC databases. The analysis was done by using Enrichr. Transcription factors with *P*-values < 0.05 are shown. **(d)** Fold changes of the expression levels for the genes shown in Fig 4, C in Regnase-1 deficient cells compared with WT cells. *Sp1* is not shown because it had been excluded from the analysis due to low RPKM values. **(e)** Luciferase reporter assay for analyzing Regnase-1 mediated suppression of gene expression through the 3´UTR sequence of the indicated genes. Either an empty plasmid, murine Regnase-1 or a nuclease-dead mutant (D141N) were transfected into HEK293 cells, and luciferase activity was measured on day 2 (n = 3) Data representative of two independent studies are shown. Student's t-test was used for the analysis.

Figure 5. Regnase-1 expression negatively correlates with the ILC2 population in human BAL.

(a) Correlation between the ratio of ILC2s among the BAL cells and Regnase-1 protein expression levels of ILC2s in BAL measured by flow cytometry. **(b, c)** Comparisons of the Regnase-1 protein expression levels of ILC2s in BAL measured by flow cytometry **(b)** or ratio of ILC2s among the BAL cells **(c)** between controls and IPF patients. **(d)** Comparisons of the ratio of ILC2s among the BAL cells between IPF patients without and with progression in 1 year after BAL. Mann-Whitney U-test and Spearman's rank correlation test were used.

Figure 6. Associations between the concentrations of ILC2s in peripheral blood and clinical indices among IPF patients.

(a) Associations between the number of ILC2s in peripheral blood and ICOS protein expression levels evaluated as MFI with flow cytometry. **(b)** Associations between the number of ILC2s in peripheral blood and %predicted forced vital capacity (%FVC, upper left), %predicted diffusion lung capacity of carbon monoxide (%DLco, upper right) or %predicted forced expiratory volume in 1 second (%FEV_1, lower). Spearman's rank correlation test was used for the analysis. **(c)** Kaplan–Meyer curve for respiratory death (left) and all-cause mortality (right). The log rank test was used for the analysis. MFI: mean fluorescence intensity.

Figure 1

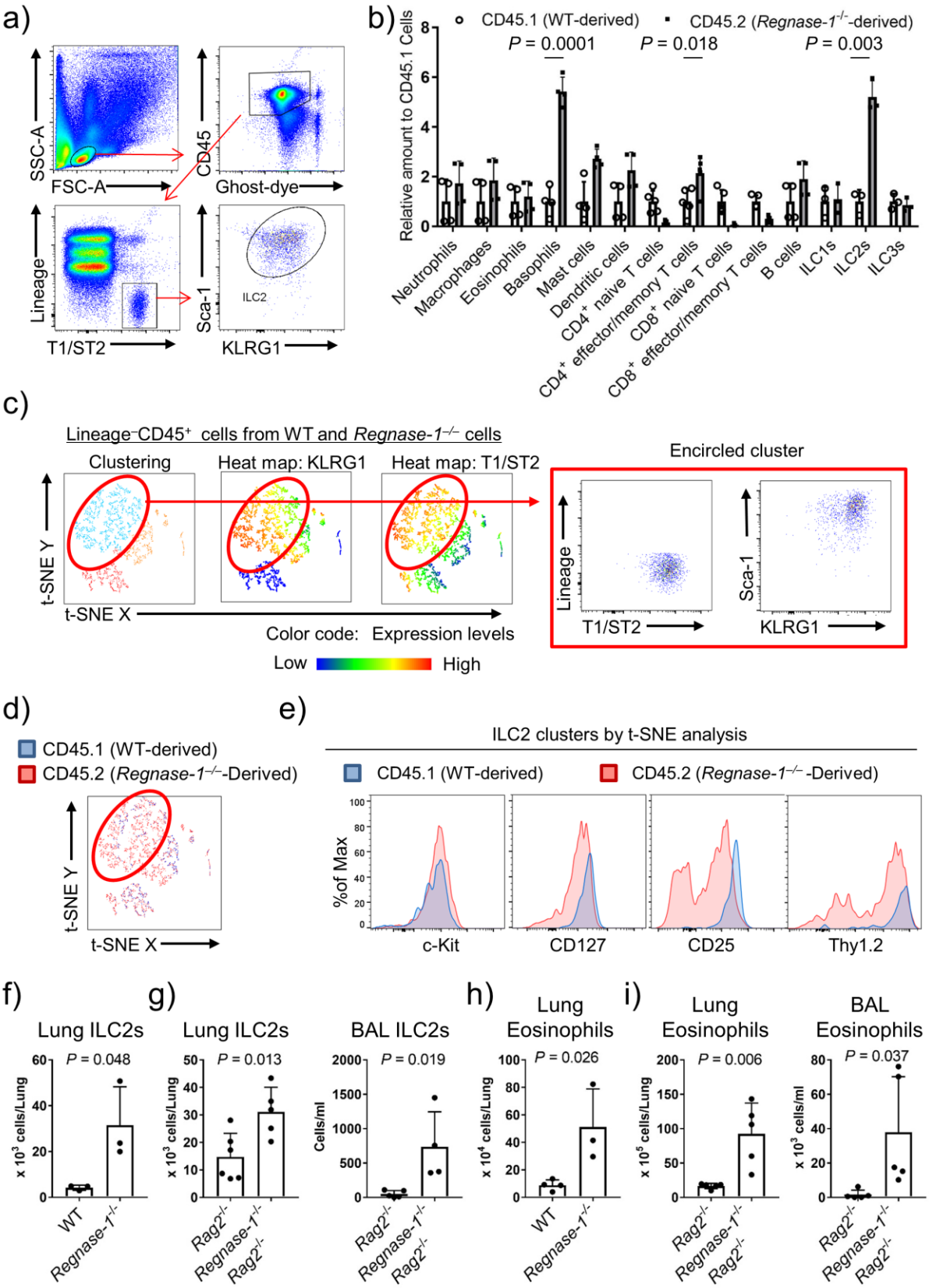
a)
SSC-A
FSC-A
CD45
Ghost-dye
Lineage
T1/ST2
Sca-1
KLRG1
ILC2
b)
CD45.1 (WT-derived)
CD45.2 (Regnase-1-/--derived)
P = 0.0001
P = 0.018
P = 0.003
Relative amount to CD45.1 Cells
Neutrophils
Macrophages
Eosinophils
Basophils
Mast cells
Dendritic cells
CD4+ naive T cells
CD4+ effector/memory T cells
CD8+ naive T cells
CD8+ effector/memory T cells
B cells
ILC1s
ILC2s
ILC3s
c)
Lineage−CD45+ cells from WT and Regnase-1−/− cells
Clustering
Heat map: KLRG1
Heat map: T1/ST2
t-SNE Y
t-SNE X
Color code: Expression levels
Low
High
Encircled cluster
Lineage
T1/ST2
Sca-1
KLRG1
d)
CD45.1 (WT-derived)
CD45.2 (Regnase-1−/−-Derived)
t-SNE Y
t-SNE X
e)
ILC2 clusters by t-SNE analysis
CD45.1 (WT-derived)
CD45.2 (Regnase-1−/− -Derived)
%of Max
c-Kit
CD127
CD25
Thy1.2
f)
Lung ILC2s
P = 0.048
x 10³ cells/Lung
WT
Regnase-1-/-
g)
Lung ILC2s
P = 0.013
x 10³ cells/Lung
Rag2-/-
Regnase-1-/-
Rag2-/-
BAL ILC2s
P = 0.019
Cells/ml
Rag2-/-
Regnase-1-/-
Rag2-/-
h)
Lung Eosinophils
P = 0.026
x 10⁴ cells/Lung
WT
Regnase-1-/-
i)
Lung Eosinophils
P = 0.006
x 10⁵ cells/Lung
Rag2-/-
Regnase-1-/-
Rag2-/-
BAL Eosinophils
P = 0.037
x 10³ cells/ml
Rag2-/-
Regnase-1-/-
Rag2-/-

Figure 2

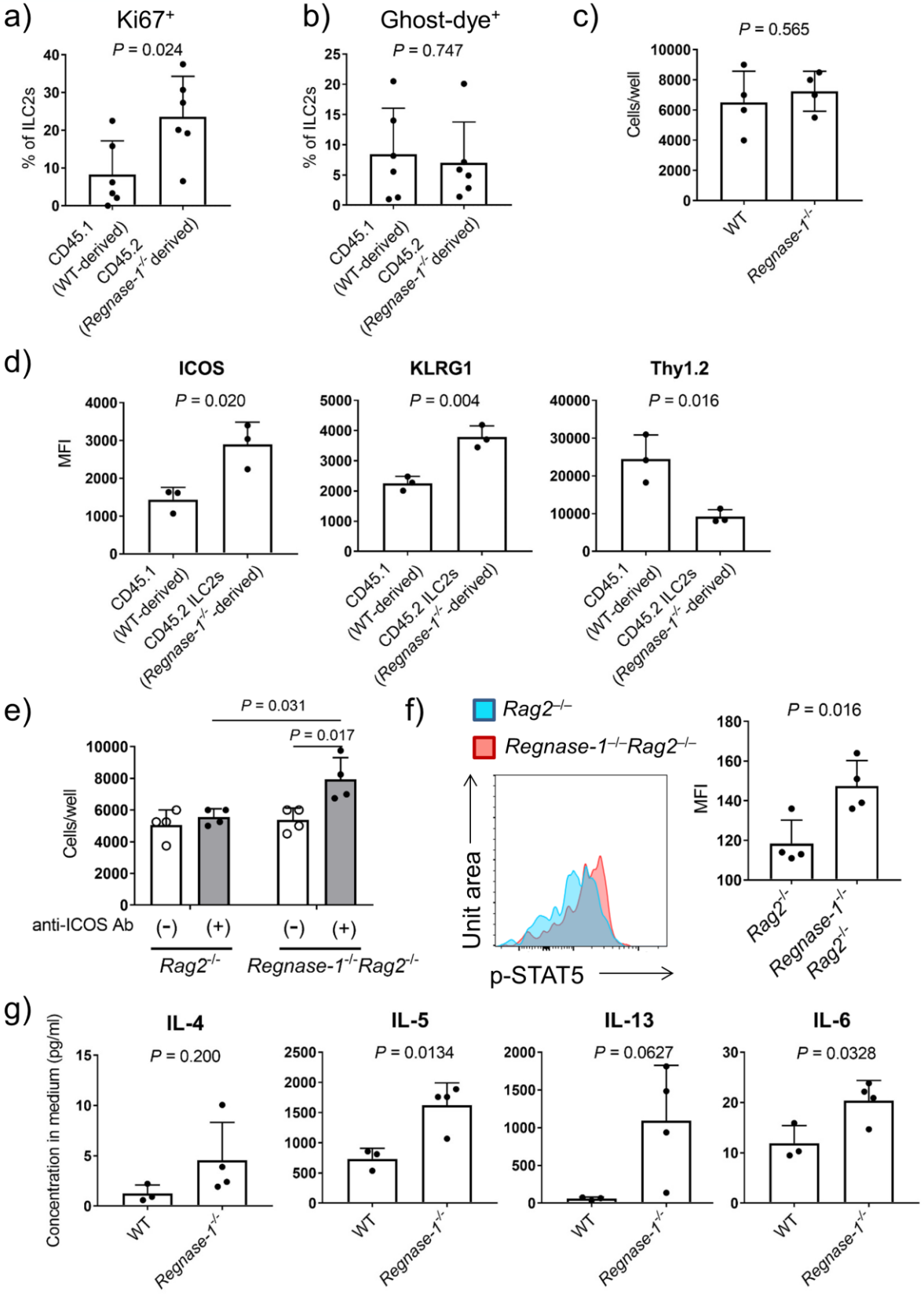
a)
Ki67+
P = 0.024
% of ILC2s
CD45.1 (WT-derived)
CD45.2 (Regnase-1-/- derived)
b)
Ghost-dye+
P = 0.747
% of ILC2s
CD45.1 (WT-derived)
CD45.2 (Regnase-1-/- derived)
c)
P = 0.565
Cells/well
WT
Regnase-1-/-
d)
ICOS
P = 0.020
KLRG1
P = 0.004
Thy1.2
P = 0.016
MFI
CD45.1 (WT-derived)
CD45.2 ILC2s (Regnase-1-/- -derived)
e)
P = 0.031
P = 0.017
Cells/well
anti-ICOS Ab
(-)
(+)
Rag2-/-
Regnase-1-/-Rag2-/-
f)
Rag2-/-
Regnase-1-/-Rag2-/-
Unit area
p-STAT5
P = 0.016
MFI
Rag2-/-
Regnase-1-/- Rag2-/-
g)
IL-4
P = 0.200
IL-5
P = 0.0134
IL-13
P = 0.0627
IL-6
P = 0.0328
Concentration in medium (pg/ml)
WT
Regnase-1-/-

Figure 3

a)

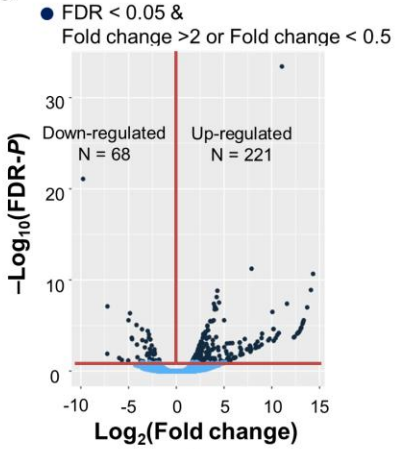

b)

Gene symbol	Log(Fold change)	FDR-*P*-value
Ccl24	13.26011	2.05E-06
Il17a	12.75751	3.01E-05
Cxcl10	8.279526	0.002946
Il4	8.231131	0.000648
Ccl6	8.226546	4.81E-05
Il6	7.820411	2.16E-11
Ccrl2	7.155005	0.000244
Il13	5.5578	0.033967
Il5	5.004657	0.002419

c)

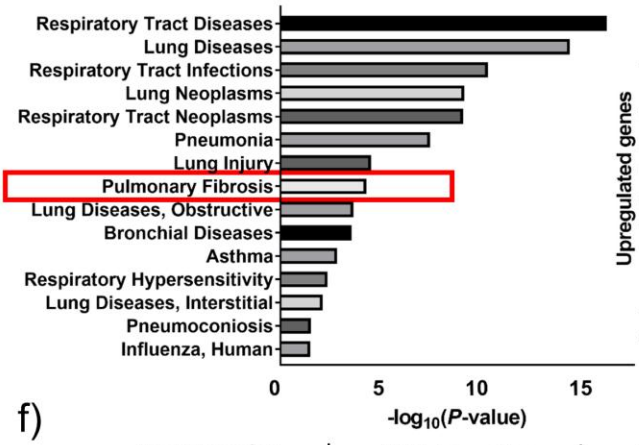

d)

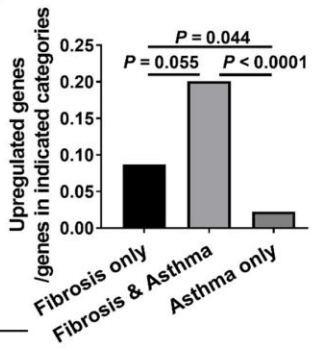

e)

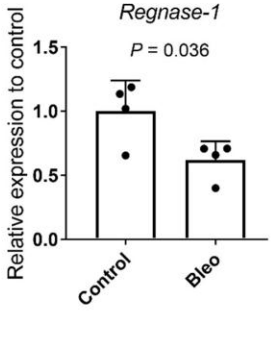

f)

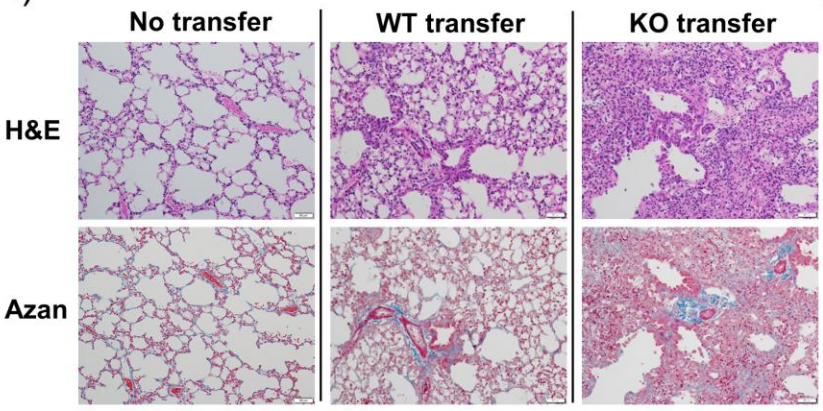

g)

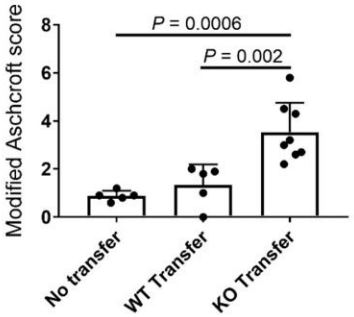

h)

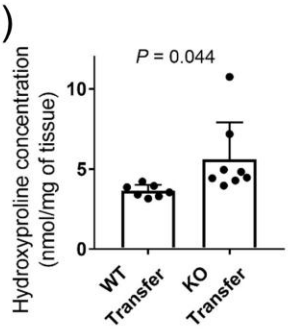

i)

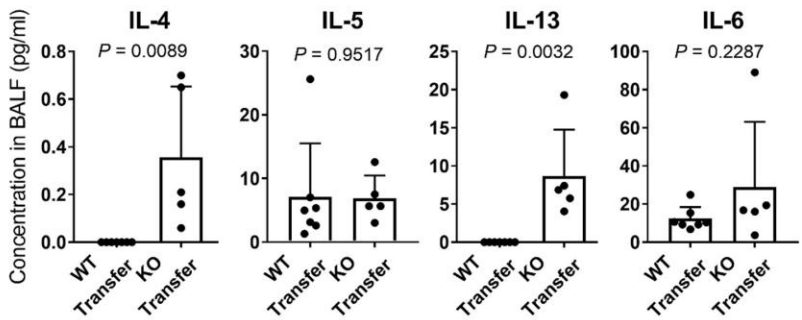

Figure 4

a)

Pathway name	*P*-value	Fold Enrichment
Cytokine Pathway	0.00243	8.07644
Gata3 Pathway	0.00781	9.04561
Cdmac Pathway	0.00943	8.48026
IL1R Pathway	0.01296	5.13955
4-1-BB Pathway	0.01321	7.53801
Tnfr2 Pathway	0.01773	6.78421
IL-5 Pathway	0.02014	12.72039
HIV Nef Pathway	0.02233	3.50907
NFkB activation by Nontypeable Hemophilus influenzae Pathway	0.03242	5.42737
MAPK Pathway	0.03384	2.72928
Cytokines and Inflammatory Response Pathway	0.03593	5.21862
Erythropoietin mediated neuroprotection through NF-kB pathway	0.03747	9.25120
IL-10 Pathway	0.04416	8.48026

b)

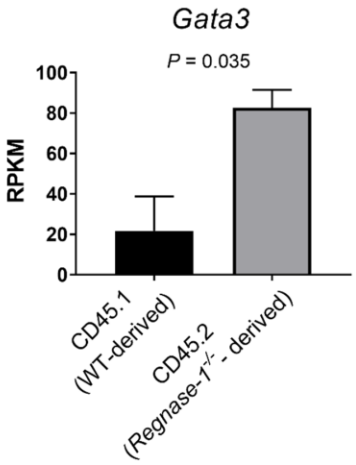

c)

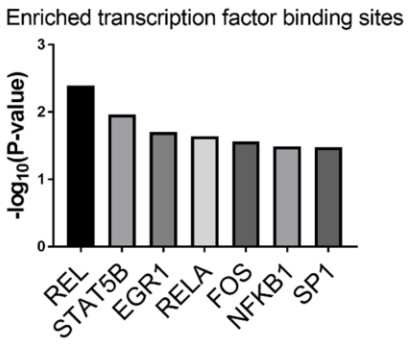

d)

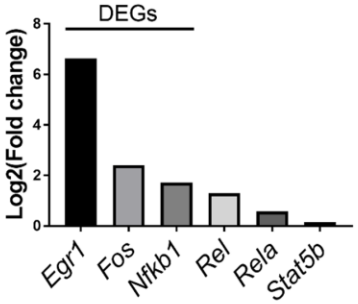

e)

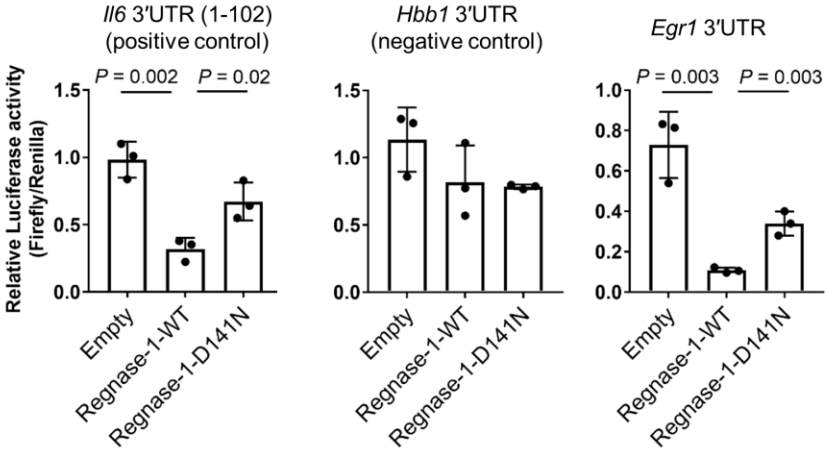

Figure 5

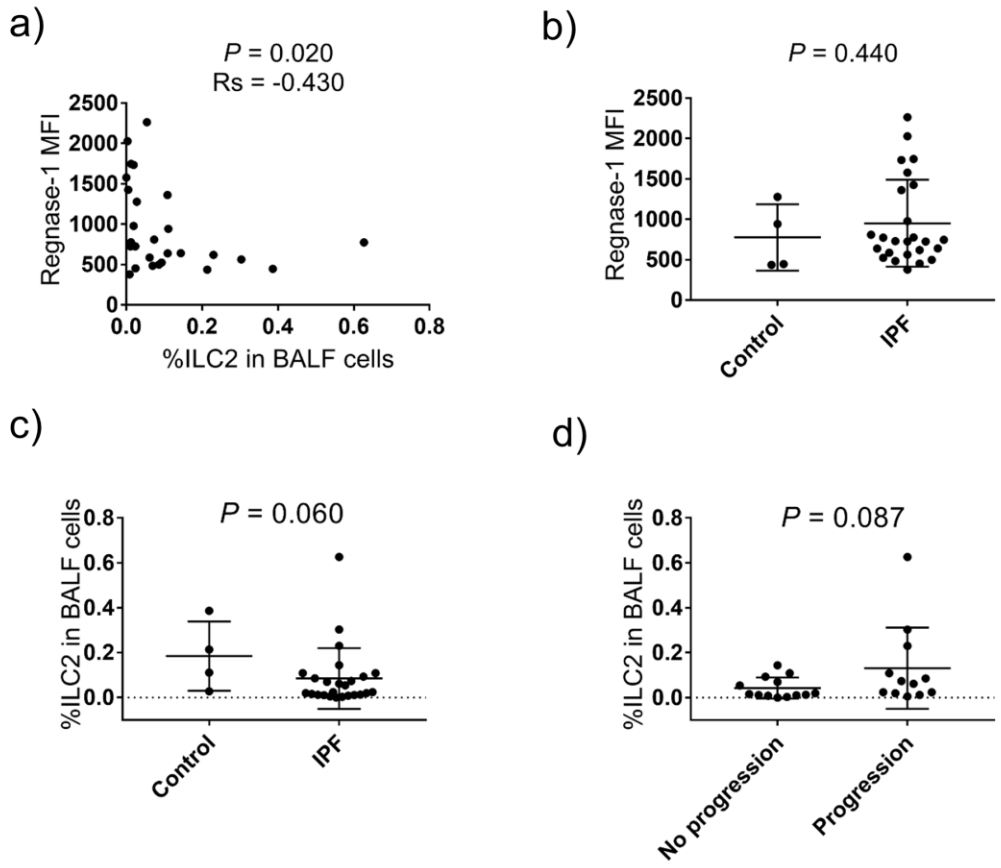
a)
P = 0.020
Rs = -0.430
Regnase-1 MFI
2500
2000
1500
1000
500
0
0.0
0.2
0.4
0.6
0.8
%ILC2 in BALF cells
b)
P = 0.440
Regnase-1 MFI
2500
2000
1500
1000
500
0
Control
IPF
c)
P = 0.060
%ILC2 in BALF cells
0.8
0.6
0.4
0.2
0.0
Control
IPF
d)
P = 0.087
%ILC2 in BALF cells
0.8
0.6
0.4
0.2
0.0
No progression
Progression

Figure 6

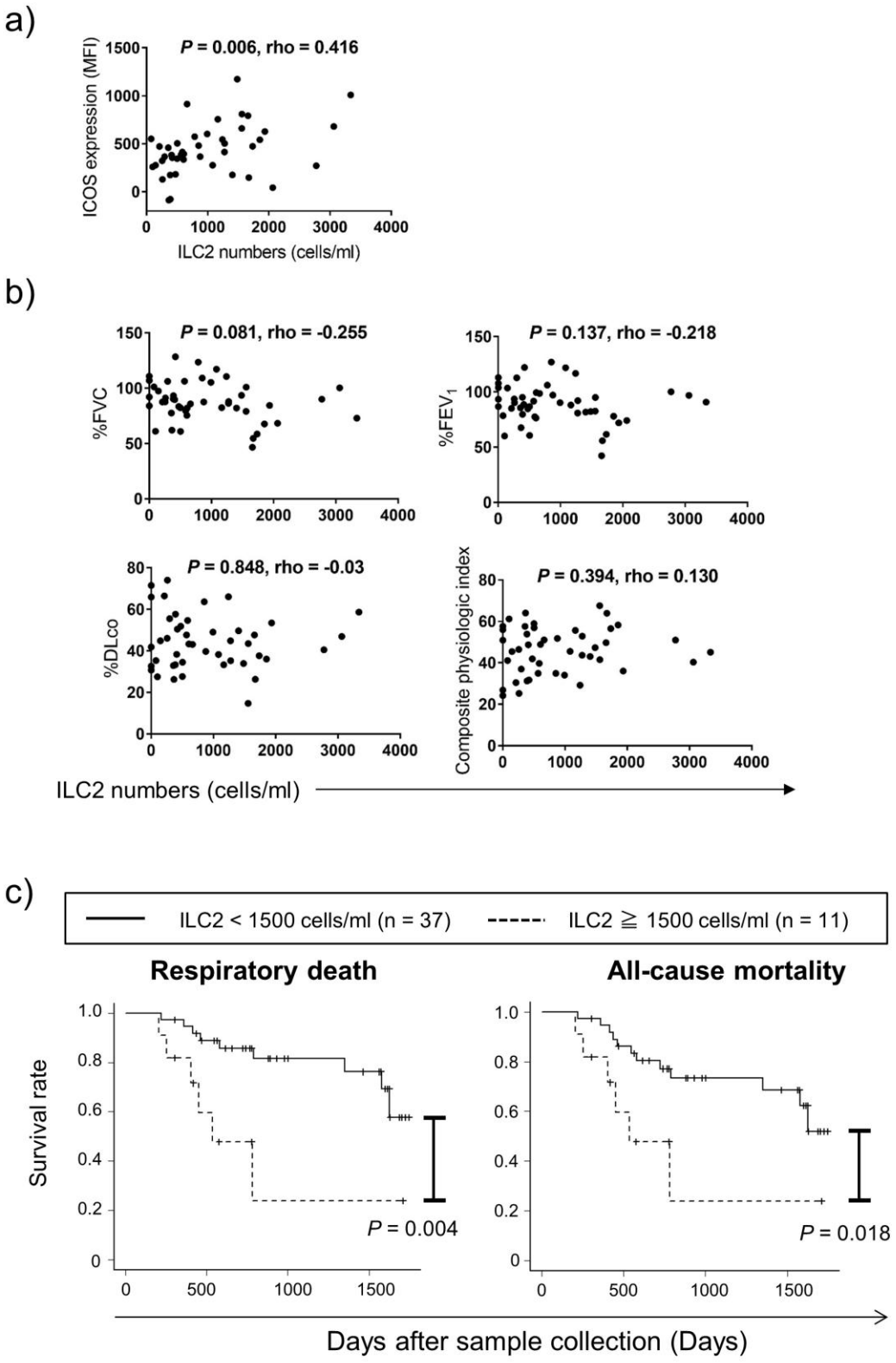
a)
P = 0.006, rho = 0.416
ICOS expression (MFI)
ILC2 numbers (cells/ml)
b)
P = 0.081, rho = -0.255
%FVC
P = 0.137, rho = -0.218
%FEV1
P = 0.848, rho = -0.03
%DLco
P = 0.394, rho = 0.130
Composite physiologic index
ILC2 numbers (cells/ml)
c)
ILC2 < 1500 cells/ml (n = 37)
ILC2 ≧ 1500 cells/ml (n = 11)
Respiratory death
All-cause mortality
Survival rate
P = 0.004
P = 0.018
Days after sample collection (Days)

Supplementary methods

Preparation of single cell suspension from the lung

Preparation of single cell suspension from the lung of mice was performed as previously described with modification[1, 2]. Briefly, lung samples were cut into pieces with scissors and put into serum-free RPMI medium supplemented with 100 μg/ml DNase I (Roche applied science) and 50 μg/ml Liberase TM (Roche applied science). After the incubation for 40 min at 37℃, EDTA solution (Nacalai Tesque) was added up to the final concentration of 10 mM, and the samples were further incubated for 10 min at 37℃. After the completion of digestion, samples were subjected to GentleMACS™ Dissociator (Miltenyi biotec), and filtered with 40 μm cell strainer. The filtered samples were centrifuged, and after the removal of supernatant, the cell pellets were treated with ACK solution to remove red blood cells. The treated samples were washed with RPMI medium containing 10% fetal bovine serum, then centrifuged, and pellets were suspended with 30% Percoll solution (GE healthcare). The suspended samples were centrifuged for 20 minutes with 2000 rpm at 20 ℃, and the cell pellets were subjected to flow cytometry.

Flow cytometry analysis

For flow cytometry analyses, cells were stained with Ghost Dye Violet 510 reagent (Tonbo Biosciences) according to the manufacturer's instruction to exclude dead cells, and then treated with antibody cocktail solution containing anti-mouse CD16/CD32 (Biolegend) antibody and surface antigen staining antibodies. For the staining of intracellular antigens, after the completion of surface staining, cells were fixed and permeabilized with Lyse/Fix buffer and Perm Buffer I (BD Pharmingen), and stained with antibodies suspended with Perm Buffer III according to the manufacturer's indication. For the staining of human Regnase-1, permeabilized cells were incubated for one hour with anti-human Regnase-1 antibody (1'

antibody, MAB7875, R&D) suspended up to 1:100 volume/volume ratio with staining buffer, then washed with staining buffer and further incubated for one hour with 2' antibody suspended up to 1:100 ratio with staining buffer. Lymphocytes were gated in FSC-A/SSC-A scatter plot as FSC-A^{low} SSC-A^{low} cell population. ILC2s in the lungs of mice were isolated as lineage$^-$ CD45$^+$ T1/ST2$^+$ Sca-1$^+$ KLRG1$^+$ cells, and human ILC2s were isolated as lineage$^-$CD45$^+$CRTH2$^+$CD127$^+$CD161$^+$ cells (supplementary figures S1B, S6). Lineage markers for mouse included CD4, CD5, CD8a, CD3e, CD19, CD49b, Gr-1, Ter119, CD11b and CD11c. Lineage markers for human included CD3, CD16, CD19, CD14, CD56 and CD20. The antibodies used in this study are listed in supplementary table S11. Data were obtained by using LSRFotessa X-20 (BD Biosciences), and sorting was done with FACSAria III (BD Biosciences). Data were analyzed with FlowJo 10.5.3 software (FlowJo, LLC).

Competitive bone marrow transfer

Lethal irradiation (9 Gy/mouse) was performed on CD45.1 congenic mice with C57BL/6J background, and the mixed bone marrow cells consisted of C57BL/6J background *Regnase-1*$^{-/-}$ mice and CD45.1 congenic mice in 1:1 ratio were by the intravenously injected. The transfered mice were maintained with adding antibiotics (Neomycin 1mg/ml, Polymyxin B 1000 U/ml) into drinking water. Six weeks after reconstitution, the analyses were performed. Each cell type was identified as follows; neutrophils: GR-1$^+$ CD11b^{high} cells, macrophages: F4/80$^+$ cells, eosinophils: CD11c$^-$ SiglecF$^+$ cells, dendritic cells: CD11c$^+$ MHC class II^{high}SiglecF$^-$ cells, mast cells: IgE$^+$C-kit$^+$ cells, basophils: IgE$^+$C-kit$^-$ CD49b$^+$ cells, effector/memory CD4$^+$ T cells: CD4$^+$ TCRβ$^+$CD44$^+$ cells, naïve CD4$^+$ T cells: CD4$^+$TCRβ$^+$CD44$^-$ cells, effector/memory CD8$^+$ T cells: CD8$^+$ TCRβ$^+$ CD44$^+$ cells, naïve CD8$^+$ T cells: CD8$^+$TCRβ$^+$CD44$^-$ cells, Th2 cells: CD4$^+$CD3$^+$GATA3$^+$ cells, B cells: CD19$^+$ cells. ILC1s were detected as lineage$^-$ CD45$^+$ IFN-γ$^+$ lymphocytes and ILC3s were

detected as lineage^{-} CD45^{+} Rorγt^{+} lymphocytes.

t-SNE analysis and clustering

We performed t-distributed stochastic neighbor embedding (t-SNE) analysis on CD45^{+}Linage^{-} Ghost-dye^{-} population as reported previously[3] by using FlowJo 10.5.3 (FlowJo, LLC). Events within the gated population was normalized between the mice by using the random down sampling plugin with reducing events up to 1000 events/sample. Then the events in all the samples were combined by concatenating function of FlowJo, and based on the concatenated data we performed the t-SNE analysis. The t-SNE settings were as follows: Iteration 1000, Perplexity 20, Eta 200. Based on the calculated t-SNE scores (X and Y), we performed clustering by using FlowSOM plugin for FlowJo with setting the number of clusters as three[4].

Bleomycin induced pulmonary fibrosis and adaptive transfer of ILC2s

ILC2s were isolated from the lungs of *Regnase-1*$^{-/-}$*Rag2*$^{-/-}$ or control *Rag2*$^{-/-}$ mice as lineage^{-}CD45^{+}T1/ST2^{+}Sca-1^{+}KLRG1^{+} lymphocytes (fig. 1B) One week before the transfer, ex-vivo cultured ILC2s were expanded with 10 ng/ml recombinant mouse IL-2, IL-7 and IL-33 (R&D Systems, Minneapolis, Minnesota). Bleomycin sulfate (Sigma Aldrich, St. Louis, Missouri) was dissolved with PBS, and the solution was intratracheally injected to *Rag2*$^{-/-}$*Il2rg*$^{-/-}$ mice at a dose of 0.15 unit/mouse. The next day, 1.5 x 10^5 ILC2s were intratracheally transferred. The lung samples were collected on day 12 after bleomycin injection. Lung fibrosis was evaluated by using the modified Ashcroft scale [5, 6].

Ex-vivo culture of ILC2s in the lung

The sorted ILC2s were seeded on 96 well u-bottom dish at 5000 cells/well concentration, and

cultured with 200 μl of RPMI-1640 medium containing 10% volume/volume fetal bovine serum, 10 mM HEPES, 100 μM nonessential amino acids, 1 mM sodium pyruvate, 100 U/ml penicillin, 100 μg/ml streptomycin, and 50 μM 2-mercaptoethanol supplemented with 10 ng/ml recombinant mouse IL-2 and IL-7 (R&D systems). The supplementation of 10 ng/ml recombinant mouse IL-2 (R&D systems), 10 ng/ml recombinant mouse IL-7 (R&D sytems) and 10 ng/ml recombinant mouse IL-33 (R&D sytems) was done as noted in the manuscript. Culture media was changed three times a week. For the stimulation of ICOS, 3 μg/ml anti-ICOS antibody (clone: C398.4A, Biolegend) was used in reference to the previous study[7].

Hydroxyproline assay

The amount of collagen in the lung tissue was evaluated by hydroxyproline assay (Quickzyme Biosciences) according to the manufacturer's instructions. Briefly, snap-frozen lung tissue (30mg) were homogenized with 300 μl of distiled deionized water. Then, 300 μl of 12M HCl was added, mix well, and heated at 95℃ for 20 hours. Next, the samples were cooled up to room temperature, and the samples were centrifuged for 10 min at 13,000g. The supernatant was diluted with 300 μl water. Thirty-five μl of diluted samples were applied to 96-well dish and mixed with 75 μl of assay buffer, incubated for 20 minutes at room temperature, and 75μl of detection reagent was added to the well. After the incubation for 60 minutes at 60℃, the OD value was read at 570 nm.

Histological analysis

Mice were euthanized, and the lung were removed, fixed in Mildform® 10N (FUJIFILM Wako Pure Chemical Corporation, Osaka, Japan), embedded in paraffin, and cut into 4-μm-thick sections. Sections were stained with hematoxylin and eosin and Azan-Mallory.

Lung fibrosis was histologically evaluated by using the modified Ashcroft scale [5, 6]. Briefly, 10 microphotographs were taken from an Azan-Mallory-stained specimen of each mouse lung tissue at 20x magnification. Lung fibrosis of each microphotograph was graded from 0 to 8 by two histologists familiar with lung histopathology (T.T and S.A) and the average score of each mouse lung tissue was calculated.

Multiplex analysis

Culture medium and BALF samples were immediately frozen at -80 °C until analysis. Samples were analyzed according to the manufacturer's instructions by using Bio-Plex Pro Mouse Cytokine 23-plex Assay kit (M60009RDPD, Bio-Rad Laboratories) and Bio-Plex 200 system.

Luciferase reporter assay

HEK293 cells were cultured with Dalbecco-Modified Eagle's Medium (Nacalai Tesque) supplemented with 10% fetal bovine serum and 50 μM β-mercaptoethanol (Invitrogen). Regnase-1 WT and D141N mutant expressing plasmids were previously described[8-10]. For the expression of these genes in mammalian cells, pFLAG-CMV2 (SIGMA) was utilized. The 3′UTR sequence of the indicated genes were inserted in firefly luciferase expressing pGL3 promoter plasmid. With each of the constructed pGL3 promoter plasmid, either of plasmid expressing Regnase-1 WT, D141N or empty (control) was transfected simultaneously, and Renilla luciferase expressing plasmid was also transfected as an internal control. Forty-eight hours after the transfection, the cell lysate was subjected to the Dual-Luciferase Reporter Assay system (Promega). Plasmids were transfected into cells by using PEI MAX solution (Polysciences, Inc.) according to the manufacturer's instruction.

RT-qPCR analysis.

Rag2$^{-/-}$ mice were administered with 0.15 U/head bleomycin, and on the day 14 the mice were sacrificed. Mice without bleomycin treatment were used for the control. ILC2s were isolated from the lung by flow cytometry, and were lysed with TRIzol® reagent (Invitrogen). We extracted RNA from the solution, and reverse transcription was performed with ReverTra Ace qPCR RT Master Mix with gDNA remover (Toyobo) according to the manufacturer's instruction. The cDNA fragments were subjected to real-time PCR with SYBR® Green PCR Master Mix (Applied Biosystems), and evaluated by StepOnePlus Real-Time PCR System (Applied Biosystems). The following primer sequences were used: mouse *Actinb*: (forward) 5′- ggctgtattcccctccatcg-3′, (reverse) 5′-ccagttggtaacaatgccatgt-3′, mouse *Regnase-1*: (forward) 5′- cgagaggcaggagtggaaac-3′, (reverse) 5′-cttacgaaggaagttgtccaggctag -3′.

Western blot

Cells were lysed with RIPA buffer. Western blot was performed as described previously[10]. Anti-human Regnase-1 antibody (1' antibody, MAB7875, R&D) and anti-mouse/human β-actin (sc-1615; Santa Cruz) were used. Rabbit anti-mouse/human Regnase-1 antibody was described previously[9]. Luminescence data was obtained by ImageQuant LAS 4000 (GE Healthcare).

RNA sequencing analyses

Isolated ILC2s from competitively transferred mice were lysed with TRIzol (Invitrogen), and total RNA was extracted. The cDNA libraries were prepared by using SMARTer PCR cDNA Synthesis Kit (Clontech) and Nextera DNA Flex Library Prep Kit (Illumina) according to the manufacturer's instruction, and the samples were sequenced on a HiSeq 2000 system (Illumina). Ribosomal sequences were excluded by using bowtie2 (version 2.2.4), and the

reads were mapped on the murine genome (mm10) by using tophat2 (version 2.0.13). After excluding the genes with RPKM value < 10 in both of CD45.1$^+$ ILC2s and CD45.2$^+$ ILC2s, fold changes in count-per-million (CPM) and False Discovery Rate-adjusted *P*-values (FDR-*P*) were calculated by using edgeR with applying quasi-likelihood dispersion estimates[11, 12]. Differentially expressed genes (DEGs) were defined as the genes with FDR- *P* of < 0.05 and fold change of < 0.5 or > 2.0. The Comparative Toxicogenomics Database (CTD) (revision 15822) was used to analyze the associations between human diseases and DEGs[13]. The associations between the upregulated genes and pulmonary diseases was assessed by using "Respiratory Tract Diseases" category in the CTD as a reference. A list of human orthologs of mouse genes was obtained from Ensembl Biomart (version Ensembl Genes 98, GRCm38.p6), and was used to convert mouse genes to their human ortholog counterparts. Pathway analysis was performed using the CGAP BioCarta Pathway in with DAVID 6.8 Bioinformatics Resources[14, 15]..

The accessions for RNA sequencing data is as follows:DNA Data Bank of Japan (DDBJ), accession number: DRA007392.

Prediction of transcription factors associated with the gene sets

The upregulated genes categorized in "Pulmonary fibrosis" by CTD were analyzed with Enrichr[16, 17]. The screening was performed by searching transcription factor binding sites for the genes through referencing the Transfac[18] and JASPAR[19] databases, and transcription factors of mouse were extracted.

Clinical data collection

Clinical information including patients' background, laboratory tests, arterial blood gas analysis, pulmonary function tests and 6MWT at the time of sample collection were obtained.

Patients were instructed to visit hospital every 1-3 months to receive chest X-ray, laboratory test and regular interview with physician. Pulmonary function test including FVC, FEV_1 and DLco was performed every 6 months unless contraindications such as pneumothorax was not observed. The median follow-up period was 1674 days for the analysis of peripheral blood and 1241 days for the analysis of BAL, respectively. Progression was defined if any of the following event was observed: > 10% relative decline in FVC, > 15% relative decline in DLco, death or acute exacerbation of IPF. The ratio of ILC2s among lymphocytes in BAL or peripheral blood was determined using flow cytometry (BD LSR Fortessa-X20, BD Bioscience). Human ILC2s were defined as $CD45^+lineage^-CD127^+CRTH2^+CD161^+$ cells (fig. S5). Written informed consent was obtained from all participants.

Clinical sample collection and analysis

BAL was performed according to the guideline[20], and the recovered BALF was centrifuged at 1500 rpm for 5 minutes, then the pellet was stored. Peripheral blood mononuclear cells was prepared by using Ficoll Paque PLUS (GE healthcare) according to the manufacturer's instruction. Cells were suspended with CELLBANKER1 (AMSBIO) and stored at -80°C. BALF lymphocyte fraction or peripheral blood lymphocyte count evaluated as regular practice was multiplied with the ILC2s/lymphocyte ratio, thereby the ratio of BALF ILC2s or the number of peripheral blood ILC2s were calculated.

Statistical analysis

For the analyses of experimental data, either of Microsoft Excel (Microsoft corporation) or GraphPad Prism version 7.00 for Windows (GraphPad Software, La Jolla California USA) was used, and Student's t-test was performed for the comparisons between the groups.

Statistical analyses for clinical data were performed with EZR (Saitama Medical Centre, Jichi

Medical University, Saitama, Japan), which is a graphical user interface for R (The R Foundation for Statistical Computing, Vienna, Austria)[21]. A Fisher's exact test was used for the analysis of categorical variables and Mann Whitney U-test was used for the comparisons of continuous data. The log–rank test was used to evaluate the cumulative survival based on Kaplan-Meyer's curve. To evaluate the power of the cut-off value to detect poor survival, we adopted three-year survival for the calculation, because previous studies reported the median survival of IPF as three years [22-24]. We set the parameters as follows; observation period: 1080 days, the estimated three-year survival of the patients: 0.5, alpha-error: 0.05. We set the survival rate of the patients within each group according to the results of the analysis. The death due to the following reasons were regarded as "Respiratory death": chronic respiratory failure, acute exacerbation of IPF, pneumonia, pneumothorax and lung cancer. For the patients who did not experience any events or whose follow-up was lost, the follow-up period was censored at the day of the last visit. The Cox proportional hazards test was used for the multivariate analysis of survival with a stepwise selection of variables based on the Akaike information criterion. A p value of < 0.05 was considered statistically significant.

Supplementary method references

1. Moro K, Ealey KN, Kabata H, Koyasu S. Isolation and analysis of group 2 innate lymphoid cells in mice. *Nat Protoc* 2015: 10(5): 792-806.

2. Nakatsuka Y, Vandenbon A, Mino T, Yoshinaga M, Uehata T, Cui X, Sato A, Tsujimura T, Suzuki Y, Sato A, Handa T, Chin K, Sawa T, Hirai T, Takeuchi O. Pulmonary Regnase-1 orchestrates the interplay of epithelium and adaptive immune systems to protect against pneumonia. *Mucosal Immunol* 2018: 11(4): 1203-1218.

3. Cameron GJM, Cautivo KM, Loering S, Jiang SH, Deshpande AV, Foster PS,

McKenzie ANJ, Molofsky AB, Hansbro PM, Starkey MR. Group 2 Innate Lymphoid Cells Are Redundant in Experimental Renal Ischemia-Reperfusion Injury. *Front Immunol* 2019: 10(826).

4. Van Gassen S, Callebaut B, Van Helden MJ, Lambrecht BN, Demeester P, Dhaene T, Saeys Y. FlowSOM: Using self-organizing maps for visualization and interpretation of cytometry data. *Cytometry A* 2015: 87(7): 636-645.

5. Ashcroft T, Simpson JM, Timbrell V. Simple method of estimating severity of pulmonary fibrosis on a numerical scale. *Journal of clinical pathology* 1988: 41(4): 467-470.

6. Hübner R-H, Gitter W, Mokhtari NEE, Mathiak M, Both M, Bolte H, Freitag-Wolf S, Bewig B. Standardized quantification of pulmonary fibrosis in histological samples. *BioTechniques* 2008: 44(4): 507-517.

7. Arimura Y, Shiroki F, Kuwahara S, Kato H, Dianzani U, Uchiyama T, Yagi J. Akt is a neutral amplifier for Th cell differentiation. *J Biol Chem* 2004: 279(12): 11408-11416.

8. Matsushita K, Takeuchi O, Standley DM, Kumagai Y, Kawagoe T, Miyake T, Satoh T, Kato H, Tsujimura T, Nakamura H, Akira S. Zc3h12a is an RNase essential for controlling immune responses by regulating mRNA decay. *Nature* 2009: 458(7242): 1185-1190.

9. Iwasaki H, Takeuchi O, Teraguchi S, Matsushita K, Uehata T, Kuniyoshi K, Satoh T, Saitoh T, Matsushita M, Standley DM, Akira S. The IkappaB kinase complex regulates the stability of cytokine-encoding mRNA induced by TLR-IL-1R by controlling degradation of regnase-1. *Nat Immunol* 2011: 12(12): 1167-1175.

10. Mino T, Murakawa Y, Fukao A, Vandenbon A, Wessels HH, Ori D, Uehata T, Tartey S, Akira S, Suzuki Y, Vinuesa CG, Ohler U, Standley DM, Landthaler M, Fujiwara T, Takeuchi O. Regnase-1 and Roquin Regulate a Common Element in Inflammatory mRNAs by Spatiotemporally Distinct Mechanisms. *Cell* 2015: 161(5): 1058-1073.

11. Robinson MD, McCarthy DJ, Smyth GK. edgeR: a Bioconductor package for

differential expression analysis of digital gene expression data. *Bioinformatics* 2010: 26(1): 139-140.

12. McCarthy DJ, Chen Y, Smyth GK. Differential expression analysis of multifactor RNA-Seq experiments with respect to biological variation. *Nucleic Acids Res* 2012: 40(10): 4288-4297.

13. Davis AP, Grondin CJ, Johnson RJ, Sciaky D, McMorran R, Wiegers J, Wiegers TC, Mattingly CJ. The Comparative Toxicogenomics Database: update 2019. *Nucleic Acids Res* 2019: 47(D1): D948-d954.

14. Huang da W, Sherman BT, Lempicki RA. Systematic and integrative analysis of large gene lists using DAVID bioinformatics resources. *Nat Protoc* 2009: 4(1): 44-57.

15. Huang da W, Sherman BT, Lempicki RA. Bioinformatics enrichment tools: paths toward the comprehensive functional analysis of large gene lists. *Nucleic Acids Res* 2009: 37(1): 1-13.

16. Chen EY, Tan CM, Kou Y, Duan Q, Wang Z, Meirelles GV, Clark NR, Ma'ayan A. Enrichr: interactive and collaborative HTML5 gene list enrichment analysis tool. *BMC bioinformatics* 2013: 14: 128.

17. Kuleshov MV, Jones MR, Rouillard AD, Fernandez NF, Duan Q, Wang Z, Koplev S, Jenkins SL, Jagodnik KM, Lachmann A, McDermott MG, Monteiro CD, Gundersen GW, Ma'ayan A. Enrichr: a comprehensive gene set enrichment analysis web server 2016 update. *Nucleic Acids Res* 2016: 44(W1): W90-97.

18. Matys V, Kel-Margoulis OV, Fricke E, Liebich I, Land S, Barre-Dirrie A, Reuter I, Chekmenev D, Krull M, Hornischer K, Voss N, Stegmaier P, Lewicki-Potapov B, Saxel H, Kel AE, Wingender E. TRANSFAC and its module TRANSCompel: transcriptional gene regulation in eukaryotes. *Nucleic Acids Res* 2006: 34(Database issue): D108-110.

19. Khan A, Fornes O, Stigliani A, Gheorghe M, Castro-Mondragon JA, van der Lee R,

Bessy A, Cheneby J, Kulkarni SR, Tan G, Baranasic D, Arenillas DJ, Sandelin A, Vandepoele K, Lenhard B, Ballester B, Wasserman WW, Parcy F, Mathelier A. JASPAR 2018: update of the open-access database of transcription factor binding profiles and its web framework. *Nucleic Acids Res* 2018: 46(D1): D1284.

20. Meyer KC, Raghu G, Baughman RP, Brown KK, Costabel U, du Bois RM, Drent M, Haslam PL, Kim DS, Nagai S, Rottoli P, Saltini C, Selman M, Strange C, Wood B. An official American Thoracic Society clinical practice guideline: the clinical utility of bronchoalveolar lavage cellular analysis in interstitial lung disease. *Am J Respir Crit Care Med* 2012: 185(9): 1004-1014.

21. Kanda Y. Investigation of the freely available easy-to-use software 'EZR' for medical statistics. *Bone Marrow Transplant* 2013: 48(3): 452-458.

22. Raghu G, Rochwerg B, Zhang Y, Garcia CA, Azuma A, Behr J, Brozek JL, Collard HR, Cunningham W, Homma S, Johkoh T, Martinez FJ, Myers J, Protzko SL, Richeldi L, Rind D, Selman M, Theodore A, Wells AU, Hoogsteden H, Schunemann HJ, American Thoracic S, European Respiratory s, Japanese Respiratory S, Latin American Thoracic A. An Official ATS/ERS/JRS/ALAT Clinical Practice Guideline: Treatment of Idiopathic Pulmonary Fibrosis. An Update of the 2011 Clinical Practice Guideline. *Am J Respir Crit Care Med* 2015: 192(2): e3-19.

23. Kim HJ, Perlman D, Tomic R. Natural history of idiopathic pulmonary fibrosis. *Respir Med* 2015: 109(6): 661-670.

24. Richeldi L, Varone F, Bergna M, de Andrade J, Falk J, Hallowell R, Jouneau S, Kondoh Y, Morrow L, Randerath W, Strek M, Tabaj G. Pharmacological management of progressive-fibrosing interstitial lung diseases: a review of the current evidence. *Eur Respir Rev* 2018: 27(150).

Supplementary figure S1. Competitive bone marrow transfer and Identification of mouse ILC2s

A. Schematic picture for the competitive BM transfer model. **B.** Ratio of a $CD45.1^+$ (WT mice derived) and $CD45.2^+$ (*Regnase-1*$^{-/-}$ mice derived) Th2s in the lung of competitive bone marrow transfer model mice (n = 5).

Supplementary figure S2. Tissue-specificity of Regnase-1-mediated control of ILC2s

Ratio of a $CD45.1^+$ (WT mice derived) and $CD45.2^+$ (*Regnase-1*$^{-/-}$ mice derived) ILC2s in mesenteric fat-associated lymphoid cells (n = 5). Data are shown as mean ± SD. Student's t-test was used for analyses.

Supplementary figure S3. Regnase-1 deficiency affects the number of eosinophils in the lung

Flow cytometry analysis of the population of eosinophils among live cells in *Rag2*$^{-/-}$ mice and *Regnase-1*$^{-/-}$ *Rag2*$^{-/-}$ mice.

Supplementary figure S4. The characterization of *Regnase1*-deficient ILC2s

Cell surface expression levels of the indicated proteins on the ILC2s in the lung of *Rag2*$^{-/-}$ and *Rag2*$^{-/-}$ *Regnase1*$^{-/-}$ mice (n = 5). Expression levels were evaluated by flow cytometry. Data are shown as mean ± SD. Student's t-test was used for analyses. MFI: mean fluorescence intensity.

Supplementary figure S5. *Regnase1*-deficient ILC2s promote pulmonary fibrosis

A. Top 15 human diseases that were associated with the human ortholog counterparts of upregulated genes. Comparative Toxicogenomics Database (CTD) analyzer was utilized for

the analysis. **B.** Schematic figure of the adaptive transfer of ILC2s into bleomycin-induced pulmonary fibrosis model mice. ILC2s sorted from the lungs of *Rag2*$^{-/-}$ mice or *Regnase-1*$^{-/-}$ *Rag2*$^{-/-}$ mice were cultured in the presence of 10 ng/ml IL-2 and IL-7 for 7 to 14 days, then expanded in the presence of 10 ng/ml IL-2, IL-7 and IL-33 for 7 days. On the day following intratracheal injection of 0.15 unit/head bleomycin, 1.5 x 10^5 cultured ILC2s were intratracheally transferred, and the samples were collected on day 12.

Supplementary figure S6. Identification of human ILC2s

Representative gating strategy picture for human ILC2s by flow cytometry. Human ILC2s were identified as CD45$^+$Lineage$^-$CRTH2$^+$CD161$^+$IL-7R$^+$ cells. Doublet depletion was done by the analysis of FSC-A/FSC-H and SSC-A/SSC-H.

Supplementary figure S7. Evaluation of human Regnase-1 protein by flow cytometry

A. Western blot for the cell lysate prepared from WT and *Regnase-1*-deficient Jurkat cells using anti-human Regnase-1 antibody MAB7875. The red arrow indicates the signal for Regnase-1. **B.** Flow cytometry histogram (upper) and dot plot (lower) comparing the fluorescence intensity between WT (red) and *Regnase-1*-deficient (blue) Jurkat cells. **C.** Flow cytometry histogram (upper) and dot plot (lower) comparing the fluorescence intensity between human peripheral blood ILC2s treated with primary antibody (MAB7875) plus secondary antibody (red) and secondary antibody only (blue).

Supplementary figure S8. Regnase-1 expression negatively correlates with the ILC2 number in human BAL.

Correlation between the number of ILC2s among the BAL cells and Regnase-1 protein expression levels of ILC2s in BAL measured by flow cytometry. Spearman's rank correlation

test was used for analysis.

Supplementary figure S9. The clinical significance of ILC2 number in peripheral blood of in IPF patients

A. The associations between ILC2 number in peripheral blood and the indicated plasma cytokine levels in IPF patients. Spearman's rank correlation test was used for analysis. **B.** A Receiver Operating Curve was drawn to determine the optimal cutoff value of the number of ILC2s in peripheral blood to identify IPF patients who died due to respiratory causes. The area under the curve was 0.645. Several values were tested, and 1557 cells/ml was determined to be the cutoff value.

Supplementary figure S10. A graphical summary of the findings in this study

Regnase-1 expressed in ILC2s in the lung of mice suppresses the expression of ICOS, GATA3 or EGR-1 through the destabilization of the mRNAs coding these proteins, thereby restrict the proliferation and the expression of genes associated with pulmonary fibrosis. Also in human, the decrease in Regnase-1 protein levels correlated with the increase in ILC2 population in BAL, and the increased number of ILC2s was an independent factor for worse survival in IPF patients. These data suggest that Regnase-1 inhibits promotion of lung fibrosis by suppressing pro-fibrotic function of ILC2s both in mouse and human.

Supplementary figure S1

A

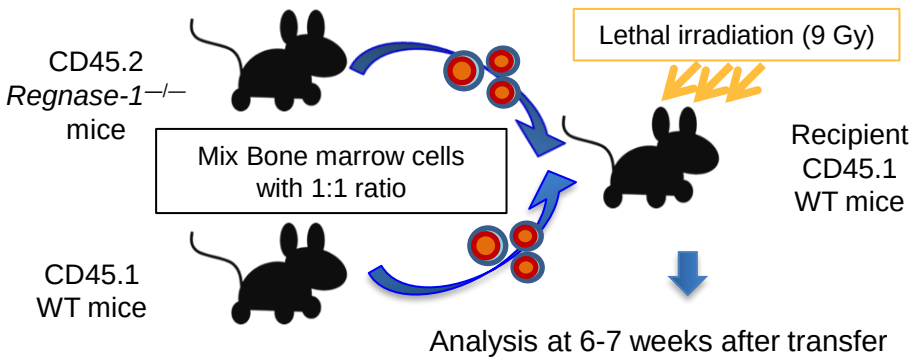

B

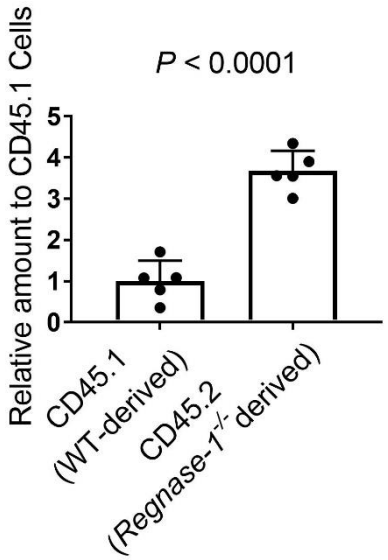

Supplementary figure S2

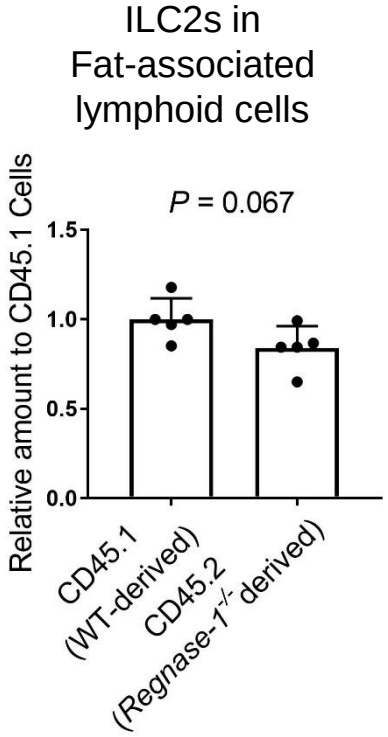

Supplementary figure S3

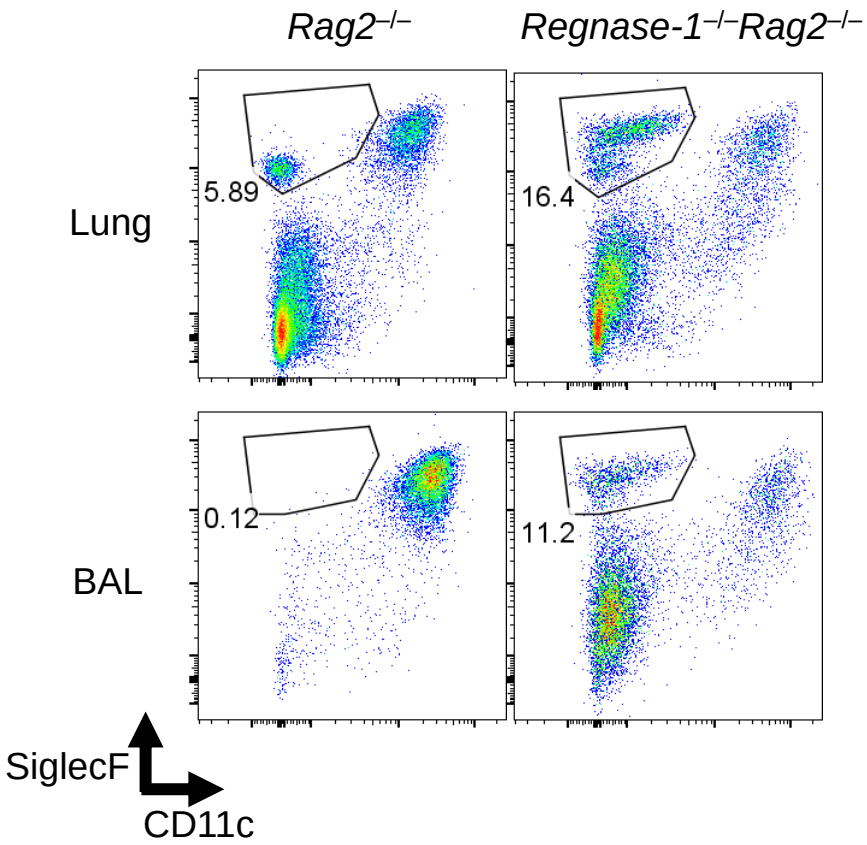

Supplementary figure S4

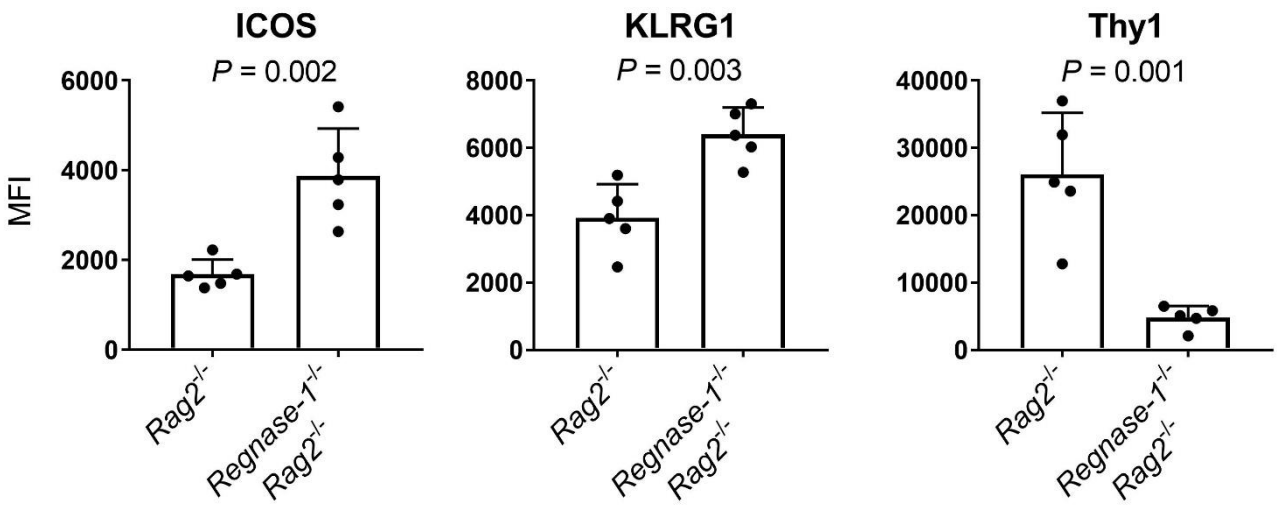

Supplementary figure S5

A

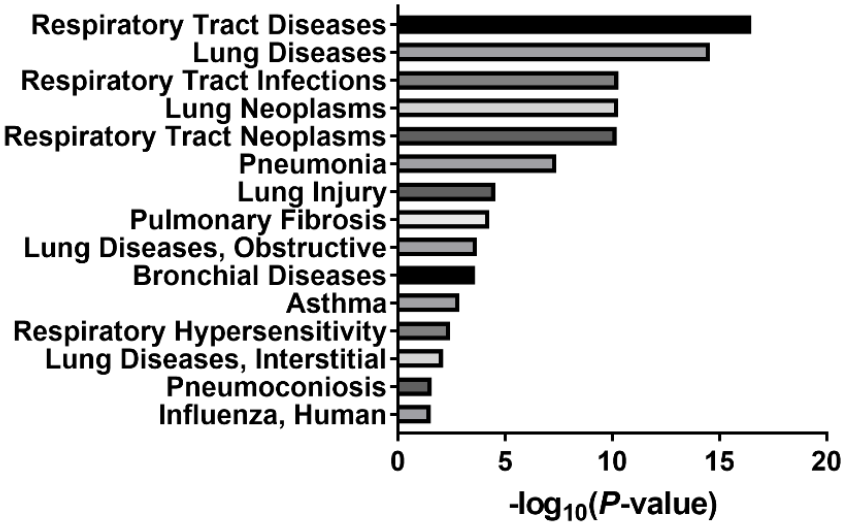

B

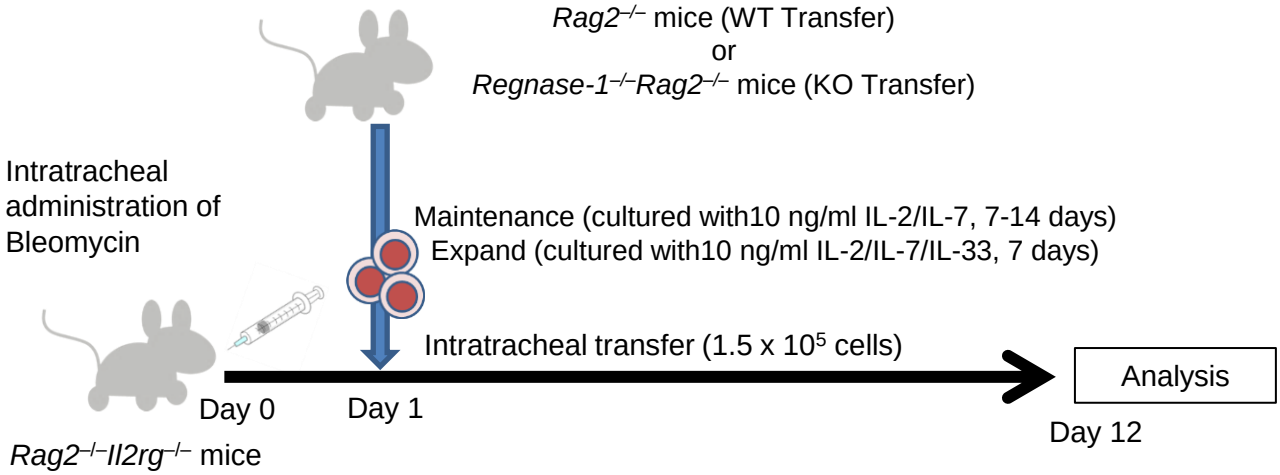

Supplementary figure S6

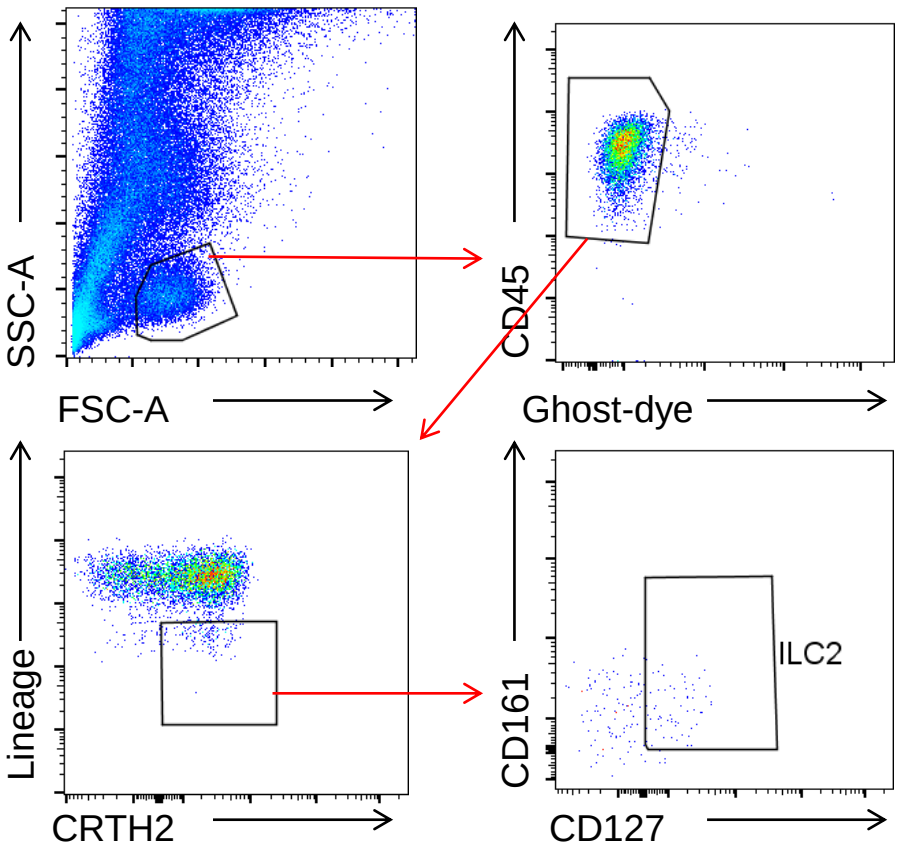

Supplementary figure S7

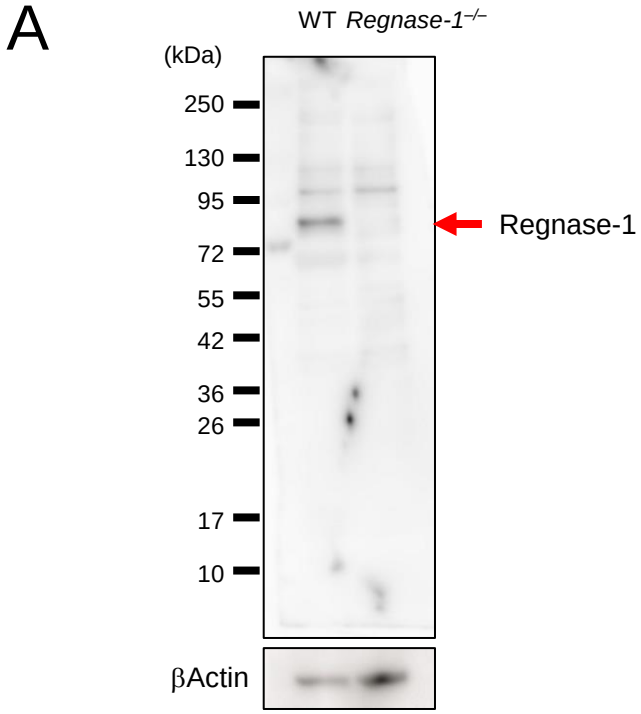

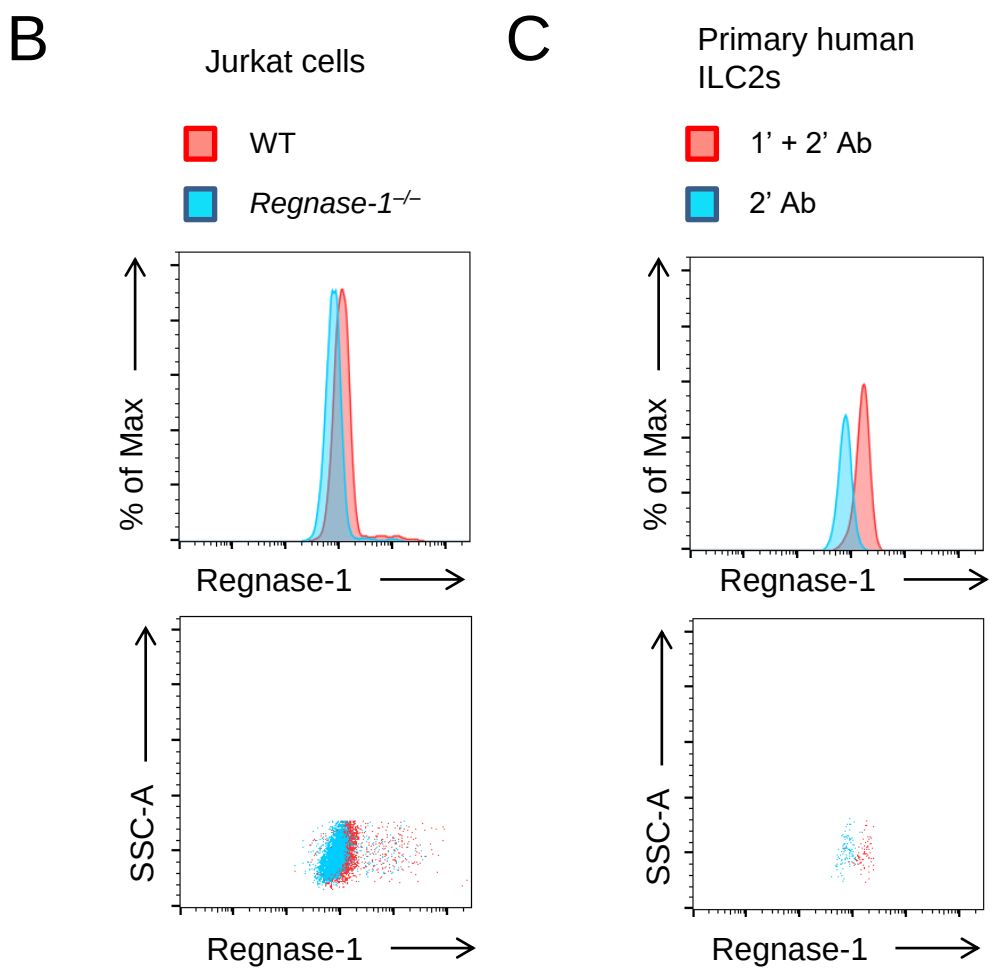

Supplementary figure S8

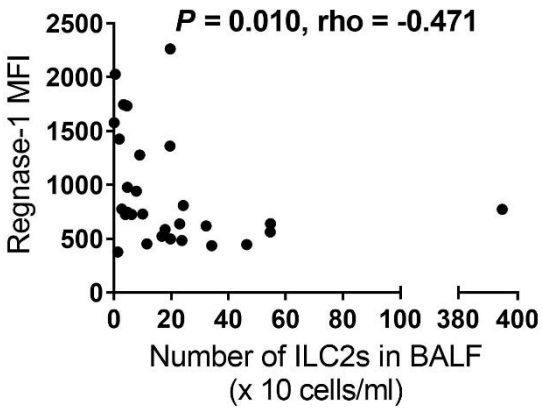

Supplementary figure S9

A

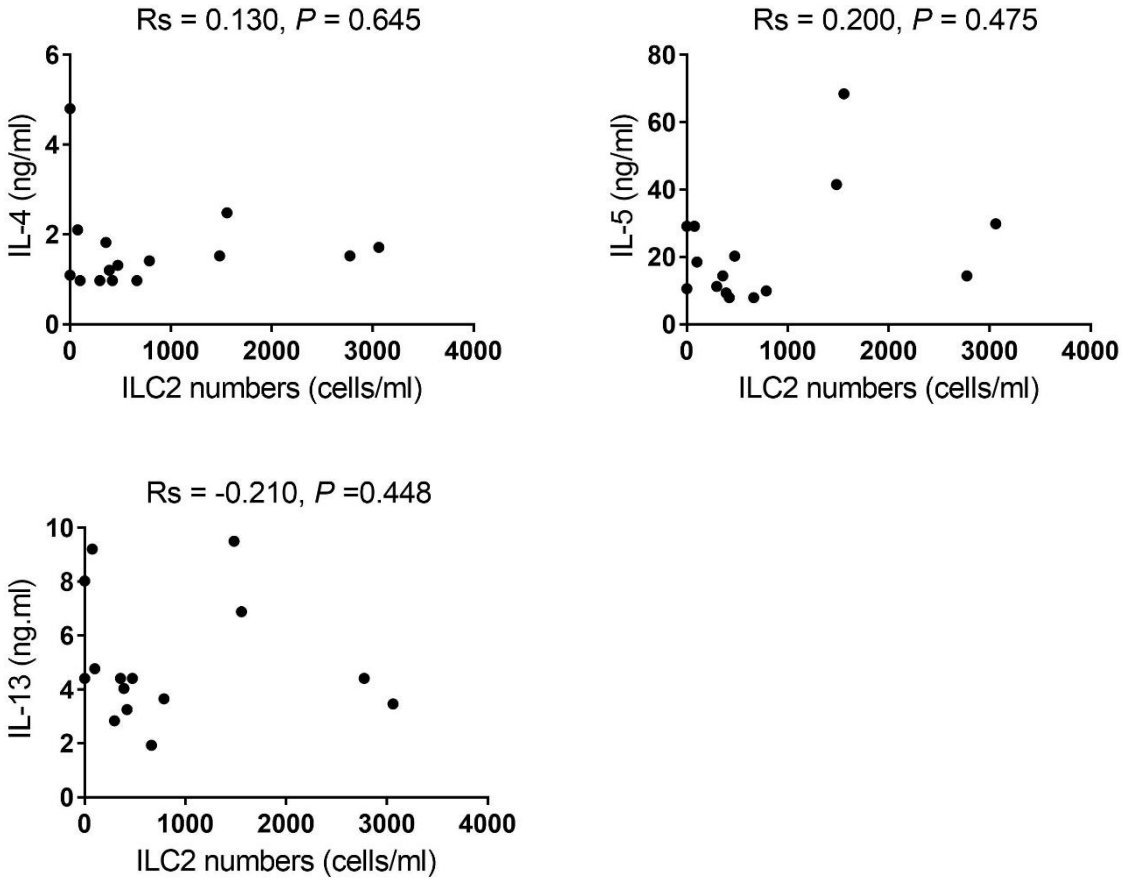

B

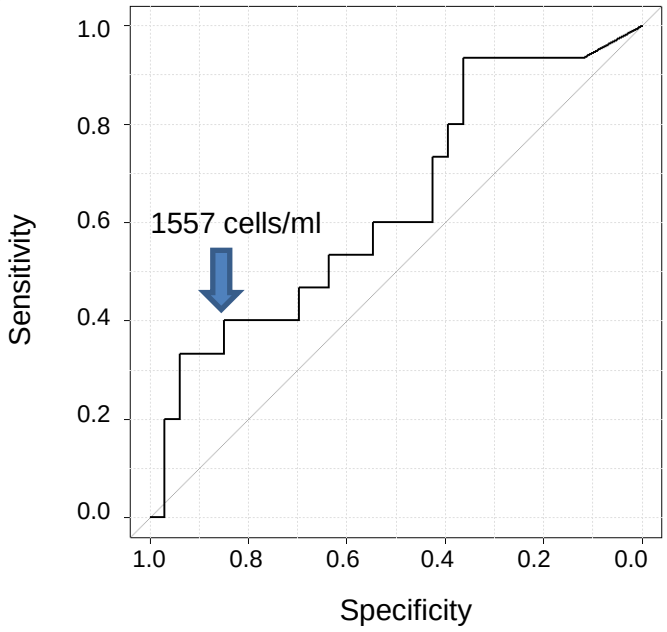

Supplementary figure S10

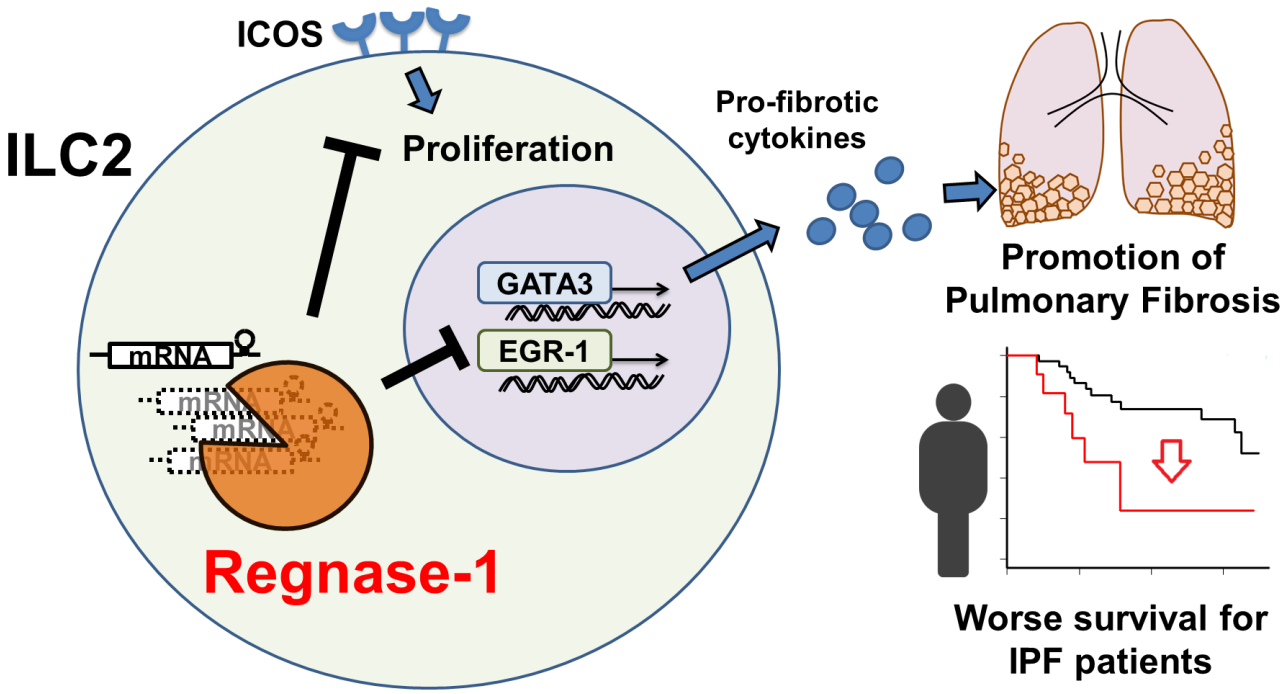

Supplementary table S9. Background of study cases in the analysis of BAL

	Control	IPF
Number	4	25
Male sex (%)	2 (50.0)	21 (84.0)
Age, years	54.00 [18.00, 62.00]	71.00 [46.00, 83.00]
Pirfenidone use, n	NA	12 (48.0)
Corticosteroid use, n	NA	5 (20.0)
Nintedanib use, n	NA	8 (32.0)
Regnase-1 expression in BAL ILC2s	694.00 [437.00, 1279.00]	730.00 [378.00, 2264.00]
BAL ILC2 ratio, %	0.16 [0.03, 0.39]	0.02 [0.00, 0.63]
BAL cell_number, cells/□l	140.00 [70.00, 320.00]	260.00 [130.00, 630.00]
BAL Eosinophils, %	0.00 [0.00, 0.00]	2.00 [0.00, 11.00]
BAL Lymphocytes, %	16.50 [10.00, 19.00]	11.00 [0.00, 67.00]
BAL Monocytes, %	82.00 [78.00, 88.00]	82.00 [30.00, 99.00]
BAL Neutrophils, %	1.50 [0.00, 5.00]	3.00 [0.00, 16.00]
Never smoker, n	NA	3 (12.0)
Former smoker, n	NA	21 (84.0)
Current smoker, n	NA	1 (4.0)
Brinkman index	NA	550.00 [0.00, 1800.00]
PaO_2, mmHg	NA	86.70 [62.80, 108.00]
$PaCO_2$, mmHg	NA	39.20 [33.10, 49.80]
%DLco, %	NA	56.94 [32.85, 93.75]
$\%FEV_1$, %	NA	85.70 [48.50, 131.00]
%FVC, %	NA	83.80 [50.30, 134.50]
Composite Physiologic Index	NA	39.45 [13.17, 59.70]
KL-6, U/ml	NA	720.00 [288.00, 3138.00]
SP-D, ng/ml	NA	230.50 [17.20, 1000.00]
Progression in one year, n	NA	12 (48.0)
Death, n	NA	9 (36.0)

FVC: forced vital capacity, DLco: diffusion lung capacity of carbon monoxide,

FEV_1: forced expiratory volume in one second

6MWT: 6-minute walk test, SpO_2: saturation of peripheral O_2

PaO_2: partial pressure of O_2 $PaCO_2$: partial pressure of CO_2

Data are shown as number (%) or median [range].

Fisher's exact test and Mann-Whitney U-test were used for analyses.

Supplementary table S10. Causes of deaths

	ILC2 ≦1500 (n = 12)	ILC2 > 1500 (n = 6)	*P*-value
Respiratory death			
Chronic respiratory failure	0 (0.0)	3 (50.0)	0.025
Pneumonia	3 (25.0)	0 (0.0)	0.515
Lung Cancer	1 (8.3)	2 (33.3)	0.245
Acute exacerbation of IPF	5 (41.6)	1 (16.7)	0.600
Non-Respiratory death			
Sudden death/ Heart attack	1 (8.3)	0 (0.0)	> 0.99
Urinary tract infection	1 (8.3)	0 (0.0)	> 0.99
Not clear	1 (8.3)	0 (0.0)	> 0.99

Data are shown as number (%). Fisher's exact test was used for the analyses.

Supplementary table S11. Antibodies used in this study

Antibody	Clone	Distributor
FITC-conjugated anti-mouse CD4	GK1.5	Biolegend
FITC-conjugated anti-mouse CD5	53-7.3	Biolegend
FITC-conjugated anti-mouse CD8a	53-6.7	Biolegend
FITC-conjugated anti-mouse CD3e	145-2C11	BD Pharmingen
FITC-conjugated anti-mouse CD19	6D5	Biolegend
FITC-conjugated anti-mouse CD49b	DX5	Biolegend
FITC-conjugated anti-mouse Gr-1	RB6-8C5	Biolegend
FITC-conjugated anti-mouse Ter119	Ter119	Biolegend
FITC-conjugated anti-mouse CD11b	M1/70	Biolegend
FITC-conjugated anti-mouse CD11c	N418	Biolegend
FITC-conjugated anti-mouse IgE	RME-1	Biolegend
PE-conjugated anti-mouse T1/ST2	U29-93	BD Pharmingen
APC-conjugated anti-mouse CD45	30-F11,	Tonbo biosciences
APC-conjugated anti-mouse phospho-STAT5	SRBCZX	eBioscience
APC-Cy7-conjugated anti-mouse/human KLRG1	2F1	Biolegend
PE-Cy7-conjugated anti-mouse Sca-1	D7	Biolegend
PerCP-Cy5.5-conjugated anti-mouse CD45.2	clone 104	Biolegend
Biotin-conjugated anti-mouse CD45.1	A20	Biolegend
FITC-conjugated anti-human lineage cocktail 1 (CD3, CD16, CD19, CD14, CD56, CD20)	SK7, 3G8, SJ25C1, MφP9, NCAM16.2, L27	BD Pharmingen
PE-conjugate anti-human CRTH2	BM16	Biolegend
APC-conjugated anti-human CD127	A019D5	Biolegend
APC-Cy7-conjugated anti-human CD45	2D1	Biolegend
BV421-anti-human CD161	HP-3G10	Biolegend
BV421-conjugated Streptavidin		Biolegend